Millimeter Wave Imaging Architecture for On-The-Move Whole Body Imaging

Borja Gonzalez-Valdes, *Member, IEEE*, Yuri Álvarez, *Senior Member, IEEE*, Yolanda Rodriguez-Vaqueiro, *Student Member, IEEE*, Ana Arboleya-Arboleya, Antonio García-Pino, *Senior Member, IEEE*, Carey M. Rappaport, *Fellow, IEEE*, Fernando Las-Heras, *Senior Member, IEEE*, and Jose A. Martinez-Lorenzo, *Member, IEEE*

***Abstract*—This paper presents a novel interrogation system that combines multiple millimeter wave transmitters and receivers to create real-time high-resolution radar images for personnel security screening. The main novelty of the presented system is that the images can be created as the person being screened continuously moves across a corridor where the transmitters and receivers, working in a fully coherent architecture, are distributed. As the person moves, the transmitters and receivers are sequentially activated to collect data from different angles to inspect the whole body. Multiple images, similar to video frames, are created and examined to look for possible anomalies such as concealed threats. Two-dimensional (2-D) and three-dimensional (3-D) setups have been simulated to show the feasibility of the proposed system. The simulation results in 2-D have been validated using measurements.**

***Index Terms*—Backpropagation imaging, checkpoint, fast Fourier transform (FFT), imaging systems, multistatic radar system.**

I. Introduction

In homeland security applications, there is an increasing demand for methods to improve personnel screening for concealed object and contraband detection at security checkpoints. In this context, active nearfield millimeter-wave (mm-wave) imaging radar systems are able to provide high-resolution imaging at an affordable cost. The object of interest is first illuminated by mm waves and then the scattered field is measured and processed to reconstruct the surface (or volume) of the object.

Manuscript received June 18, 2015; revised January 11, 2016; accepted February 18, 2016. Date of publication XXXX XX, XXXX; date of current version XXXX XX, XXXX. This work was supported in part by the Ministerio de Ciencia e Innovacin of Spain/FEDER under project MIRIIEM-TEC2014-54005-P, in part by the Gobierno del Principado de Asturias through the PCTI 2013-2017, GRUPIN14-114, in part by the Spanish Government under project TACTICA, in part by the European Regional Development Fund (ERDF), in part by the Galician Regional Government under Projects CN2012/279, CN2012/260 (AtlantTIC) and the Plan I2C (2011–2015), and in part by the Science and Technology Directorate, U.S. Department of Homeland Security under the Award Number 2008-ST-061-ED0001.

B. Gonzalez-Valdes, Y. Rodriguez-Vaqueiro, and A. García-Pino are with the Atlantic Research Center, Universidad de Vigo, 36310 Vigo, Spain (e-mail: bgvaldes@com.uvigo.es; yrvaqueiro@com.uvigo.es; agpino@com.uvigo.es).

Y. Álvarez, A. Arboleya Arboleya, and F. Las-Heras are with the Area of Signal Theory and Communications, Department of Electrical Engineering, Universidad de Oviedo, E-33203 Gijón, Spain (e-mail: yalopez@tsc.uniovi.es; aarboleya@tsc.uniovi.es; flasheras@tsc.uniovi.es).

C. M. Rappaport and J. A. Martinez are with the ALERT Center, Northeastern University, Boston, MA 02115 USA (e-mail: rappapor@ece.neu.edu; jmartine@ece.neu.edu).

Color versions of one or more of the figures in this paper are available online at http://ieeexplore.ieee.org.

Digital Object Identifier 10.1109/TAP.2016.2539372

The development of checkpoints that allow high passenger flow is becoming a priority. This has motivated the design of mm-wave imaging systems that minimize passenger inconvenience.

The International Air Transport Association (IATA) has defined several specifications that future checkpoints for personnel screening should meet. Novel paradigms in the design of the checkpoints specify that "from 2020 and beyond it is envisaged that the passenger will be able to flow through the security checkpoint without interruption unless the advanced technology identifies a potential threat," [1] (page 14).

In [1], a computer graphics design of the checkpoint of the future proposed by IATA is presented. The novelty with respect to existing architectures is the inclusion of a beltway or hallway to avoid passenger flow interruption.

Current state-of-the-art mm-wave imaging systems for security screening require people to enter and stand in front of the scanning system. Mm-wave generation and acquisition can be achieved using static arrays of transmitters and receivers [2], [3], or using movable arrays to create planar [4], [5], or cylindrical [6]–[8] acquisition domains. Most of them are based on monostatic radar and Fourier inversion [2]–[6]. Monostatic imaging systems are cost effective, but they are only able to reconstruct surfaces that create specular reflection and they are not well suited for imaging scattering objects with sudden profile variations [9]. Further, they are prone to dihedral artifacts as described in [8], [10], and [11].

Based on the new checkpoint architecture proposed by the IATA, this paper introduces a novel concept for mm-wave scanning system for personnel screening. The proposed imaging system does not include any mechanical movement, and whole body imaging is obtained taking advantage of the movement of the person under test when passing through the system on a moving walkway.

The main contribution of this paper is the introduction of this novel architecture, called on-the-move imaging [12], [13], that, to the best of the author's knowledge, has not been previously conceived nor demonstrated.

This paper is structured as follows. Section II describes the proposed mm-wave screening system. Imaging algorithm for multistatic setups is briefly described in Section III. Proof-of-concept is validated through two-dimensional (2-D) simulation

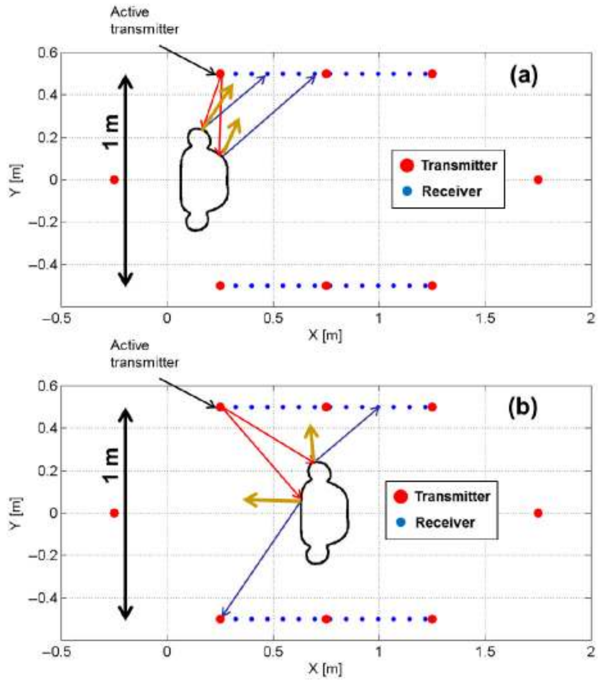

Fig. 1. On-the-move imaging concept. OUT movement between the two walls of radar antennas provides multiple points-of-view for every transmitter and receiver, thus increasing multistatic information. (a) and (b) represent two different OUT positions within the hallway.

examples in Section IV, and measurement results in Section V. Extension to two-dimensional (3-D) whole human body imaging is described and validated in Section VI. Finally, the conclusion is presented in Section VII.

II. On-the-Move Hallway Concept

The novel mm-wave on-the-move imaging system for personnel screening takes advantage of: 1) the movement of the person when passing through the imaging system and 2) a multistatic radar configuration, where some of the transmitters and receivers are separated with a subtended angle relative to the person equal or greater than 90° to capture information from all possible wave incident and scattering angles.

A top view of the suggested multistatic architecture is plotted in Fig. 1. Several transmitters (red dots) and receivers (blue dots) are placed on the sides of the hallway. The person moves along the security checkpoint on a moving walkway.

The imaging radar system takes advantage of multiple incidence angles that illuminate different areas of the person depending on the active transmitter and the placement of the person within the hallway, as illustrated in Fig. 1. A single transmitter can illuminate different areas of the person while crossing the hallway. Reciprocally, the scattered field is collected by different receivers depending on the transmitting element and the current position of the person. This is illustrated with the red and blue arrows in Fig. 1 that represent direct reflection contributions given by the incident angle and the normal to the surface according to Snell's law.

Multistatic information can be incremented by placing transmitters at the hallway ends. For practical implementation, this would partially block the persons path. This is solved in the 3-D case placing the receivers at the hallway ends below and above the moving walkway.

For every transmitter, the scattered field is collected on the receiving arrays placed on the hallway sides, and for every receiving array, a reflectivity image is recovered. The reflectivity images associated with each transmitter are coherently combined. This configuration assumes that, for a single position, the body remains still while all the transmitters are sequentially activated and the scattered field is collected by the receivers. In this sense, and since the acquisition on the receivers can be done in parallel, the use of a low number of transmitters is desirable. A fully electronic scanning system similar to the one in [3] would easily allow for such an acquisition procedure.

A critical aspect in the design of the imaging system is the selection of the frequency band. Table I shows a comparison among the proposed hallway concept and some of the existing mm-wave scanning systems. It can be observed that, for a given size of the scanner, higher frequency bands provide better cross-range resolution, at the expense of losing dynamic range due to free-space propagation losses. Furthermore, clothing becomes less transparent for these higher frequency bands, and radiofrequency hardware becomes more expensive. The work presented in [5] addresses the aforementioned drawbacks introducing an ultra-wideband (UWB) imaging system. In addition to the improved range resolution and dynamic range, the novelty of this study is the fact that the sampling rate can be relaxed by taking advantage of grating lobes cancellation in UWB arrays, which will be of interest concerning practical implementation of the on-the-move architecture.

TABLE I
Comparison With State-of-the-Art mm-Wave Imaging Systems

Reference	Scanning area (cm)[1]	PSF (mm)[2]	Frequency band (GHz)	Number of antennas
On-the-move	100×200[3]	10×10	15 – 30	2×80601 Rx 60 Tx
UWB MIMO array, [5]	50×130	10×10	2.8 – 19.5	4 Tx 8 Rx, Height motion.
Flat 2-D array, [2]	100×200	3.0×1.5	72 – 80	3072 Tx 3072 Rx
Linear array, vertical movement [4]	72.6 Movable 2 m in height	10.0×3.8	27 – 33	66 Tx, 66 Rx, Height motion

[1]Scanning area size: width ×height.
[2]PSF (point spread function): range ×cross range.
[3]Receiving panels size.

III. Imaging Algorithm

Practical mm-wave scanning system implementation demands real-time imaging capabilities. Standard backpropagation techniques [14] require millions of calculations for electrically large acquisition and imaging domains. To illustrate the numerical magnitude of the problem, typical values for acquisition points and imaging voxels are 10^5 and 10^7, respectively, assuming an operational frequency of 30 GHz ($\lambda = 1$ cm) and sampling every half wavelength in both domains according to Nyquist criterion.

The reflectivity function on a volumetric domain $\rho_t(x', y', z')$ can be recovered from the scattered field $E^t_{scatt}(f, x, z)$ acquired on a flat receiving aperture placed at $y = Y_0$, by solving the following integral equation [9], [14], when the tth (with t from 1 to N_{tx}) of a group of transmitters is active

$$\rho_t(x', y', z') = \iiint E^t_{scatt}(f, x, z) e^{+jk((x-x')^2+(Y_0-y')^2+(z-z')^2)^{1/2}} e^{+jk((x^t_{inc}-x')^2+(y^t_{inc}-y')^2+(z^t_{inc}-z')^2)^{1/2}} df\,dx\,dz \quad (1)$$

where $(x^t_{inc}, y^t_{inc}, z^t_{inc})$ denotes the position of the tth point source-like transmitter, $k = 2\pi f/c$, y-axis is the range axis (depth), x- and z-axes are horizontal and vertical cross ranges, and f is the frequency.

Fast propagation techniques, such as the inverse fast multipole method, have been proposed [15], reducing the calculation time by several orders of magnitude. Moreover, (1) can be parallelized taking advantage of GPU hardware. However, these solutions are still too computationally expensive for applications requiring real-time imaging.

Fourier-based techniques have been widely used in monostatic setups for real-time imaging [3]–[5], thanks to the fact that plane wave incidence can be considered during the inversion. Multistatic setups require different Fourier processing as the transmitter and receiver are placed in different positions. A novel Fourier-based imaging technique, totally suitable for the proposed hallway-based on-the-move imaging system, is presented in [9]. The idea is to decompose the imaging domain in smaller regions where an incident spherical wave can be locally treated as a plane wave. Imaging calculations for every region can be carried out in parallel, without jeopardizing the required real-time capabilities of the multistatic imaging system.

When multiple transmitters are used, the final reconstruction for a certain voxel placed in (x', y', z') can be obtained by combining the images generated by each transmitter as

$$\rho(x', y', z') = \sum_{t=1}^{N_{tx}} \rho_t(x', y', z'). \quad (2)$$

This formulation assumes all the transmitters and receivers work in a fully coherent configuration using a clock signal that provides common phase reference.

IV. 2-D Results

The proposed on-the-move imaging is first validated using a 2-D example. The frequency band ranges from 15 to 30 GHz, sampled every 300-MHz frequency steps and providing 1-cm range resolution. Two 1-m width lateral arrays of receivers with 50 evenly spaced elements are placed at $Y_0 = -0.6$ m and $Y_0 = 0.6$ m . Five transmitters are interleaved among each panel of receivers, thus resulting in $N_{tx} = 10$ transmitters. The described layout is plotted in Fig. 2. The essential aspect is that, in order to image the entire body surface, for every transmitter, receivers on both walls must receive the scattered waves (not just those adjacent to a given transmitter.)

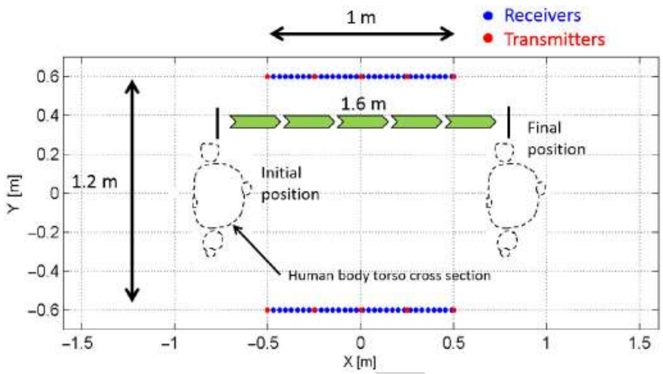

Fig. 2. 2-D example layout. OUT is displaced from position $x = -0.8$ m to $x = +0.8$ m, in five steps ($N_{pos} = 5$). 5 Tx and 50 Rx per side are considered.

The object under test (OUT) models the cross section of a human body torso (for a more realistic simulation, arms, and waist are not connected), with three attached objects on it represented as protrusions on the front, back, and arm. The object in the front is an elliptical cross-sectional metallic object. Dielectric objects ($\epsilon_r = 3.5$) are placed on the back (square cross section) and on the right arm. The OUT is displaced from the position $x = -0.8$ m to $x = 0.8$ m in 40-cm steps obtaining $N_{pos} = 5$ intermediate positions. For every position, the ten transmitters are sequentially activated and the scattered field is collected in the receiving points. A realistic composition of the human body tissue is considered [16], using a finite-difference frequency-domain (FDFD) code [17], [18] to calculate the scattered field for every transmitter and every OUT position. FDFD simulation results have confirmed that, due to the high conductivity of the skin in the frequency band of interest, the assumption that the OUT is a perfect electric conductor (PEC) is a good approximation for most cases.

The data are then used to create one reflectivity image for each intermediate position, ρ^p according to (1) and (2). The imaging domain is an $(X, Y) = (0.4, 0.6)$m rectangle, discretized in 81×121 pixels and centered in (x'_p, y'_p, z'_p). In this case, the computational cost is low and the image is recovered using the standard backprogation algorithm in (1). For every pth OUT position and tth active transmitter, the image is recovered in about 1 s using a conventional laptop (2.5-GHZ CPU and 4-GB RAM memory). As the 2-D imaging code is not parallelized yet, it takes about 50 s for the entire reconstruction.

The obtained images for two different active transmitters when the OUT is in each of the intermediate positions are presented in Fig. 3. It is clear that each transmitter allows the reconstruction of different areas of the body depending on its relative position inside the imaging system. The image obtained for the central position, combining the images created using all the transmitters according to (2), is presented in Fig. 4.

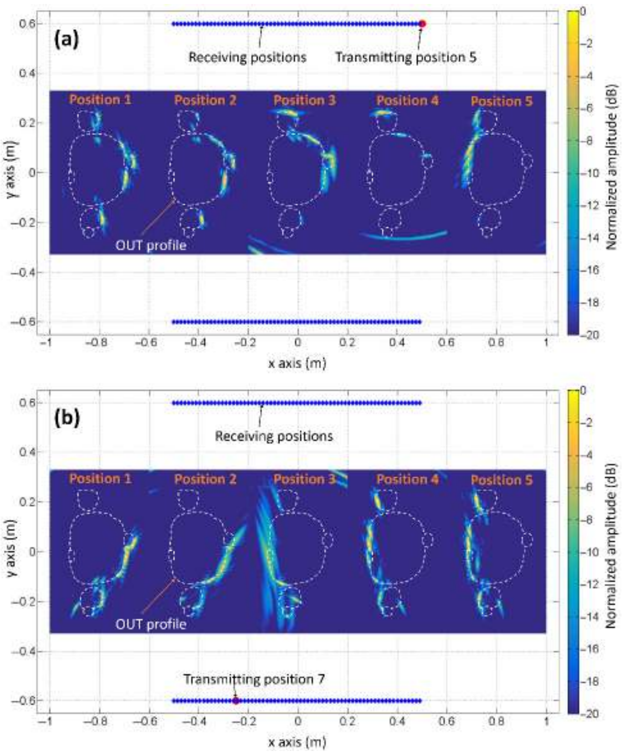

Fig. 3. Obtained images (normalized reflectivity amplitude in dB) for two different active transmitters and five intermediate positions using the setup in Fig. 2. Active transmitters are depicted as red points. Blue points represent receivers positions.

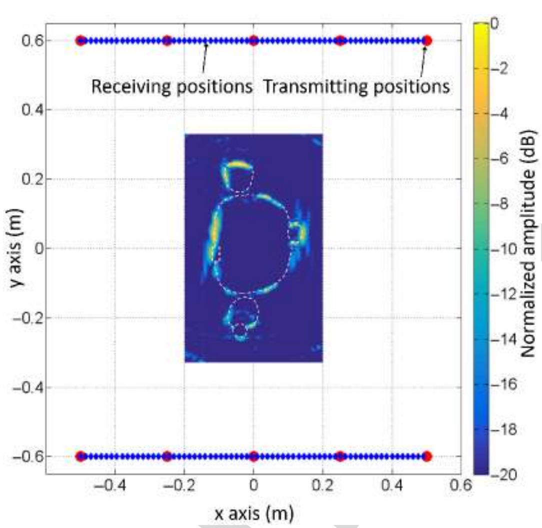

Fig. 4. Obtained image when the OUT is in the central position and the image is created using all transmitters according to (2).

The reflectivity image created by the system at each position is obtained as

$$I(x'', y'', z'') = \sum_{p=1}^{N_{pos}} |\rho(x' - x'_p, y' - y'_p, z' - z'_p)| \quad (3)$$

where the reflectivity of all the positions is centered at the origin of coordinates before being combined. Absolute value is used since the position of the OUT relative to the imaging system can slightly change from position to position, which prevents the

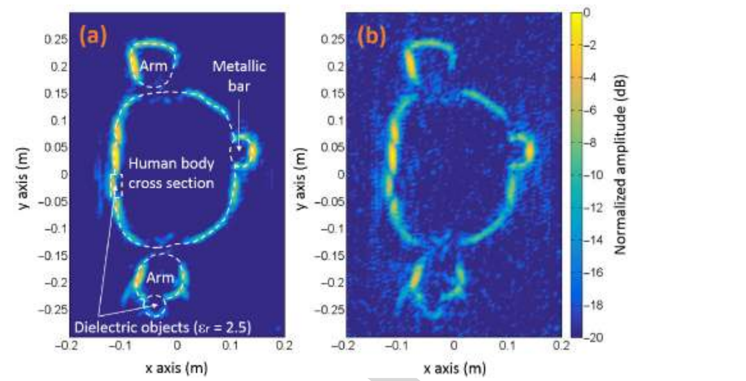

Fig. 5. Recovered OUT profile when combining in amplitude the five images (one for each position). (a) SNR = 10 dB. (b) SNR = −20 dB.

combination of the images of each position in amplitude and phase. Fig. 5 presents the final result when the five analyzed positions are combined according to (3), and when the object retains exactly the same configuration for all positions and it is only displaced in the x direction. This proves the ability of the proposed system to obtain a complete contour reconstruction. In general, the images used for threat detection in a final configuration would be the ones generated in each position as the one in Fig. 4.

Combining the information from multiple transmitters and positions also helps to increase the dynamic range of the system. Sensitivity analysis has been performed: first, the recorded signal strength in the receiving arrays for every transmitting element and OUT position has been evaluated. The case in which maximum power is recorded corresponds to the OUT at the central position illuminated by the center transmitters. The minimum power levels are recorded for the OUT in positions 1 or 5 illuminated by the closest pair of transmitters, as only a small fraction of the scattered field is collected by the arrays. The received power difference between these two cases is 11 dB.

Next, noise has been added to the field samples according to different signal-to-noise ratio (SNR) levels relative to the maximum-recorded power case. Figs. 3–5(a) correspond to SNR = 10 dB, and Fig. 5(b) to SNR = −20 dB. Thanks to the combination of multiple OUT positions and incident directions, the resulting mm-wave imaging system is able to work with low SNR.

The capability of imaging multiple users within the hallway has been also evaluated. For this purpose, the OUT placed at the center position (as in Fig. 4) is considered, but with two more OUTs (with no attached objects) at $x = 0.7$ and $x - 0.7$ m, a scenario that could correspond to a high passenger throughput situation. Due to the use of FDFD simulations, multiple reflections among OUTs are considered. Results are depicted in Fig. 6. It can be noticed that, with respect to Fig. 4, the center OUT is worse imaged due to the multipath effects. It it also possible to create the image of the front and the back of the OUTs placed at $x = 0.7$ and $x = -0.7$ m, and these results are not affected by multipath as much as the center OUT.

In order to compare this work with current state of the art systems, Fig. 7 presents the obtained image when the same contour is facing a line containing the transmitters and receivers. In

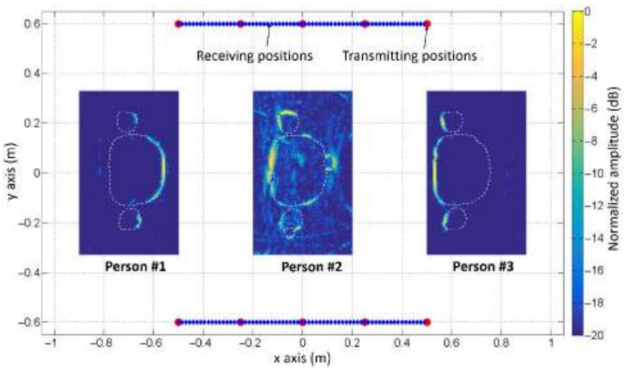

Fig. 6. Recovered image for three OUTs placed at the same time in the hallway. The image is created by combining all transmitters according to (2).

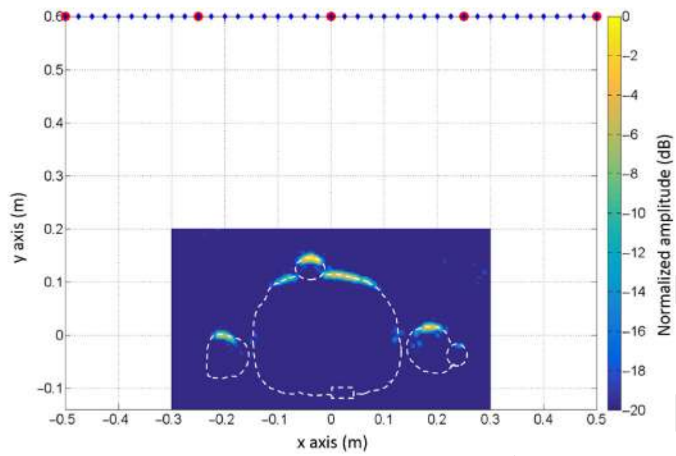

Fig. 7. Obtained image using state-of-the-art configurations where transmitters and receivers are placed in the same aperture and facing the person under test. The image is generated combining the five transmitters according to (2).

this case, different areas of the front of the contour cannot be recovered and the area that is reconstructed is much smaller than the one of Fig. 4. Concerning detection capabilities, note that the dielectric object placed on the arm is hardly detected in Fig. 7 as the energy is not scattered back to the receiving array. In the case of the on-the-move system, it can be better detected (see Figs. 4 and 5), as it is possible to find a configuration along the conveyor belt in which the energy is reflected in the dielectric-skin transition, then backscattered to one of the receiving arrays.

This 2-D example proves that, in the proposed on-the-move layout, the fact that some of the transmitters and receivers are separated with a subtended angle relative to the person equal or greater than 90° provides information from all possible wave incident angles.

V. Validation With Measurements

The proposed on-the-move imaging concept has been validated with measurements. Ka frequency band (26.5–40 GHz) has been selected to avoid hardware switching between different frequency bands. In order to ensure the maximum illumination within the hallway, WR-28 open-ended waveguides are selected as antennas.

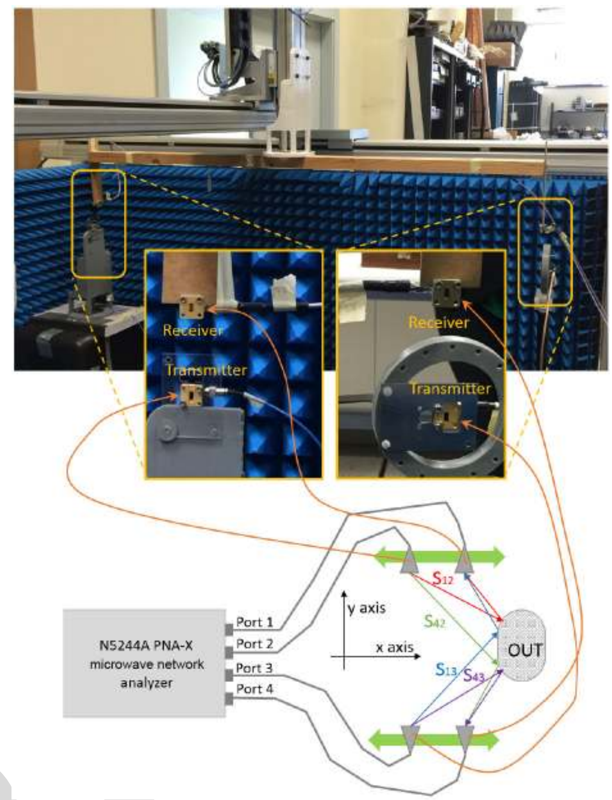

Fig. 8. Ka-band measurement system for on-the-move concept experimental validation. WR-28 open-ended waveguides are connected to the vector network analyzer ports. Receivers are mounted on a three-axis positioner.

The setup is mounted on an XYZ table measurement range [19], so some mechanical restrictions apply to the placement of the OUT, transmitters, and receiving positions (Fig. 8). In order to take advantage of the whole span of the XYZ measurement range, scattered field samples are collected in 161 points ranging from $x = -0.6$ m to $x = 0.6$ m, placed at $Y_0 = 0$ m and $Y_0 = 1.3$ m . Five transmitting positions are interleaved among the receivers, thus resulting in $N_{tx} = 10$ transmitting positions. Transmitters and receivers are separated 5 cm in height. Horizontal polarization is considered to reduce coupling between transmitter and receiver. The imaging setup is depicted in Fig. 8: two transmitters and two receivers are connected to the ports of a vector network analyzer. The power reference level is 0 dBm for all the ports. For every receiving position along the x-axis, four S-parameters are measured, as shown in Fig. 8, corresponding to the combination of each transmitter with both receivers.

The positioner of the XYZ table is used to move the receivers from each side of the hallway at the same time, as shown in Fig. 8. The pair of transmitters is manually placed at five positions along the x-axis, using the XYZ positioner as reference. For every pair of transmitting positions, acquisition time takes 3 min, and therefore, overall acquisition time for every OUT position is 15 min.

The OUT, shown in Fig. 9, is an aluminum foil-covered plastic bin with a metallic bar attached to one of the sides. Due to its translation symmetry in z-axis, it allows for 2-D analysis in an XY plane placed at ($z = h_{tx} + h_{rx}/2$), where h_{tx} is the

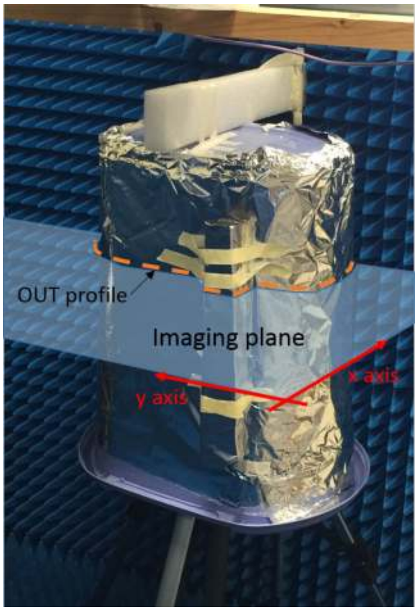

Fig. 9. Photograph of the OUT imaged with the proposed experimental setup. Receivers are mounted on a three-axis positioner.

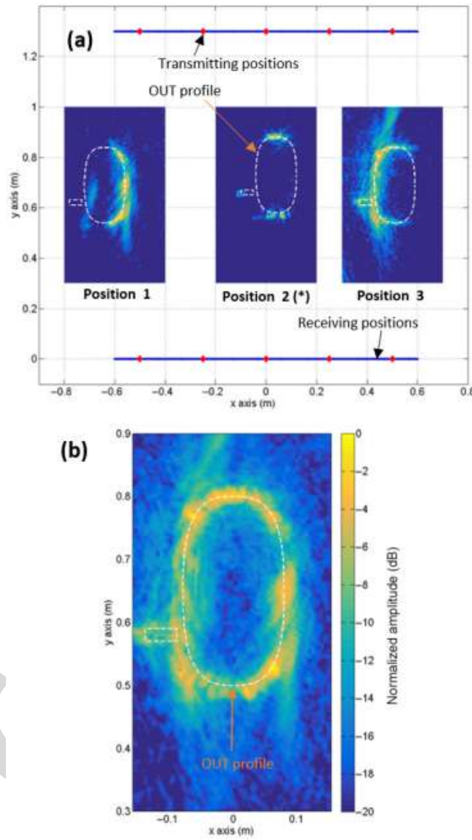

Fig. 10. Recovered OUT profile. (a) Image created on every position using all the transmitters according to (2). In the case of position 2, only the center transmitting positions ($x^t_{inc} = 0$ m) were available. (b) OUT profile when combining in amplitude the three images of (a).

height of the transmitters, and h_{rx} the height of the receivers. As mentioned in Section II, using metal to simulate the human body skin in the Ka band is an acceptable approach due to the high conductivity of the skin in mm-wave frequency bands [16]. Three positions of the OUT were considered.

The same data processing as in Section III has been applied. The image obtained for every position, combining the images created using all the transmitters according to (2), is depicted in Fig. 10(a). It can be noticed that, for positions 1 and 3, the front and the back of the OUT are imaged, and the sides of the OUT are visible for position 2.

Fig. 10(b) presents the final result combining the three OUT positions according to (3), where the OUT profile can be observed. In this case, combination is done taking the displacement of each individual image with respect to the center of the imaging domain. In practical, combination of the radar images for different positions of the person in the hallway can be based on video frames, linking video, and radar images.

In addition to the presented results, the measurement setup has been simulated, aiming to evaluate the correspondence between simulations and measurements. Results for position 2 are compared in Fig. 11. Good agreement between the reconstructed parts of the OUT for simulations and measurements is obtained.

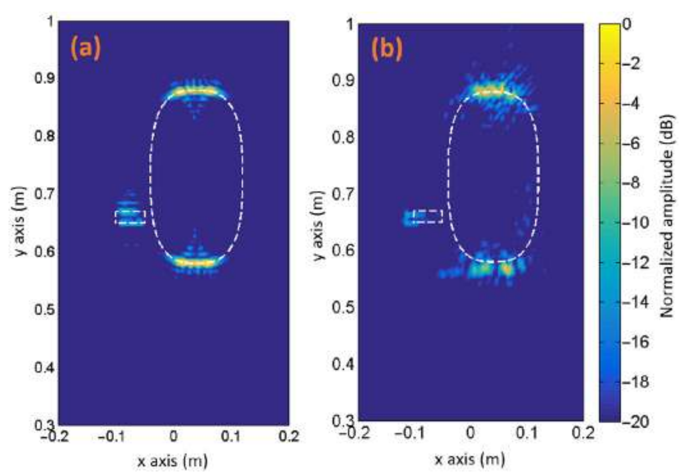

Fig. 11. Recovered OUT profile, position 2 (with center transmitting positions). (a) From simulated data. (b) From measurements.

VI. 3-D Configuration

Next, the extension from 2-D to 3-D is presented. The layout of the proposed on-the-move 3-D system is presented in Fig. 12. The setup is composed of multiple synchronized transmitters and receivers. Lateral receiving apertures of size (X, Z) = (1, 2) m, are placed at $Y_0 = 0.75$ m. The size of the panels is chosen to provide an approximated cross-range resolution of 1 cm along the z-axis and 2 cm in the x-axis.

For this preliminary setup, Nyquist sampling requirements are considered for the receiving panels, thus acquiring the field in 201×401 receiving positions per panel. Subsampling techniques as presented in [2] and [5] combined with a modified FFT algorithm for multistatic imaging with subsampled arrays can be efficiently applied in this setup to reduce the number of receivers in more than 90% [2], although this analysis is beyond the scope of this contribution. A 15-GHz bandwidth

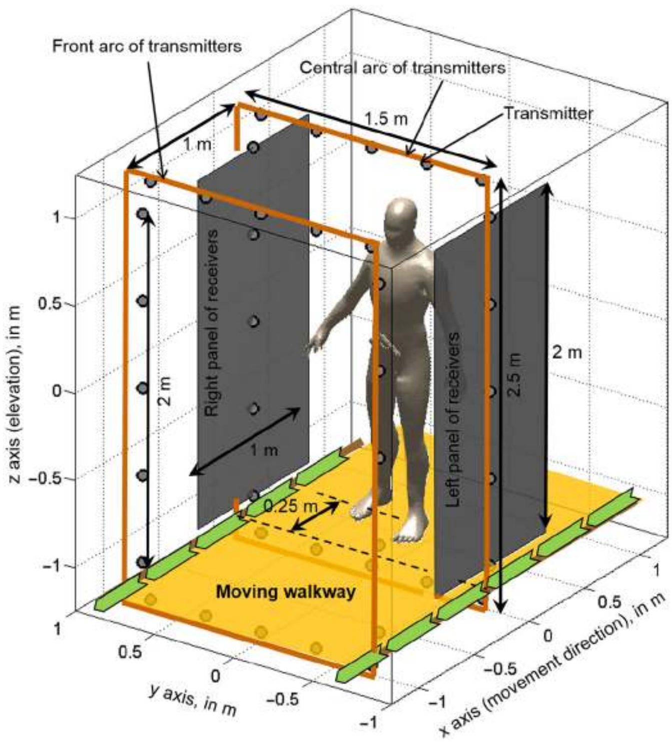

Fig. 12. Layout of the mm-wave scanner for personnel screening. For the sake of simplicity, just two arcs of transmitters, at x = 0 m, and x = −1 m, are considered. The person under test is placed at x = 0.25 m.

(BW), from 15 to 30 GHz, is chosen, similarly to the UWB imaging system described in [5]. This BW provides and approximate range resolution of 1 cm, although, for near-field radar imaging, besides the frequency and aperture size, the final system lateral and range resolutions are given by (2) and (3) of [20], respectively.

Hallway scanner dimensions have been selected to provide a resolution similar to other mm-wave scanners, as shown in Table I. It must be reminded that the number of receiving elements can be reduced in the hallway system.

Concerning processing time, the fastest operational mm-wave imaging systems listed in Table I are capable to provide detection results in less than 5 s, so the scanning process can take up to 10 s taking into account that the person needs to be placed in a particular position within the scanner. For the presented system, the overall scanning process would be limited by the time the person needs to go through the hallway.

Three arcs of transmitters, centered at x = +1, 0, and −1 m, and each having 20 elements evenly spaced along y- and z-axes, are considered. For the sake of simplicity, only the ones at −1 and 0 m, depicted in Fig. 12, will be considered to obtain the results in this section. Some of the transmitters are placed on top and below the body to ensure the areas with larger curvature (as the top of the chest and shoulders) are reconstructed.

A physical optics (PO) code [21], [22] in combination with a visibility algorithm [23] has been used to predict the parts of the body model in Fig. 12 that are illuminated by every transmitter. Also, PO provides the amount of scattered field collected on the panels. Thus, it is possible to evaluate if a certain layout of transmitters is capable of illuminating the entire person after crossing the hallway and to estimate the field scattered by the

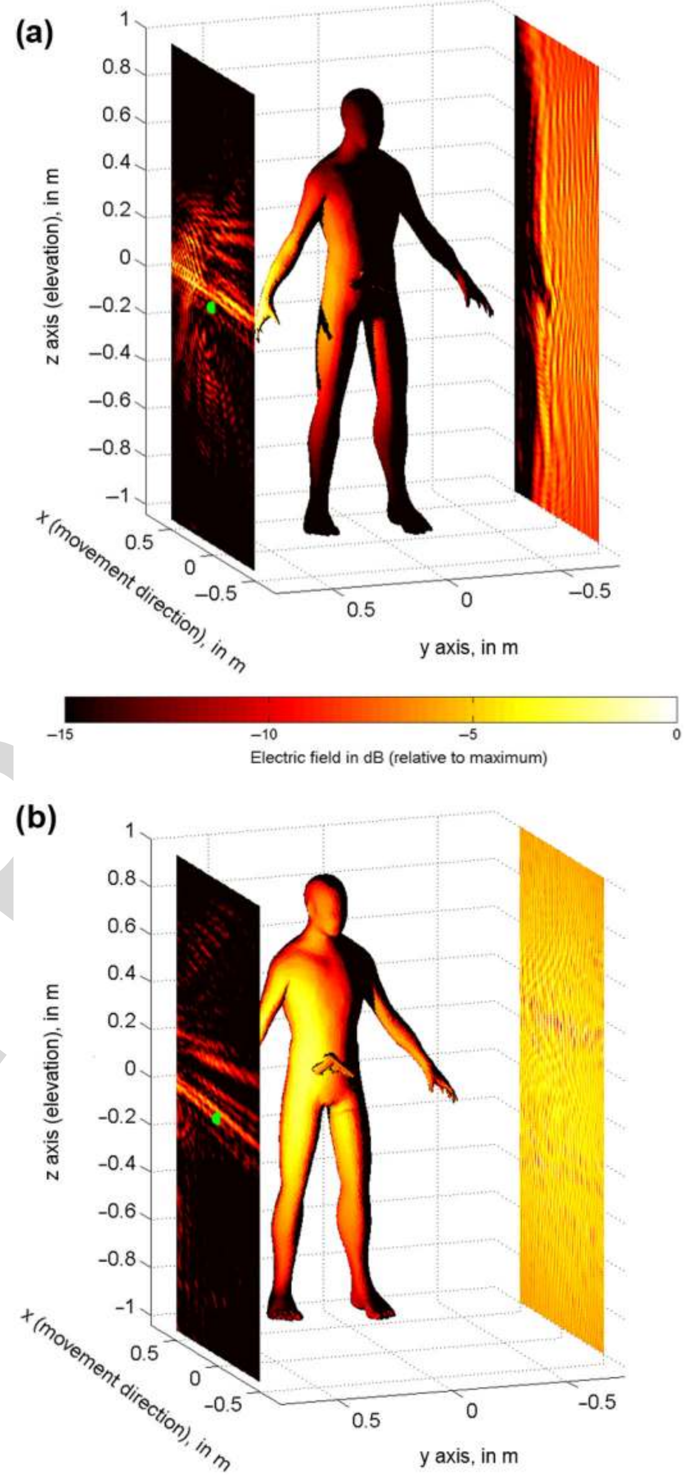

Fig. 13. Examples of human body illumination using one transmitter (highlighted in green) and scattered field on the array panels when the body model is centered in (a) 0.25 m and (b) 0.75 m.

illuminated areas on the receiving panels. For these simulations, the human body is assumed to behave as a PEC in the 15–30-GHz frequency band.

As an example, Figs. 13 and 14 show the regions of the human body under test illuminated by two different transmitters, as well as the field received on the lateral panels. Note that, even for a single position of the person in the hallway, different

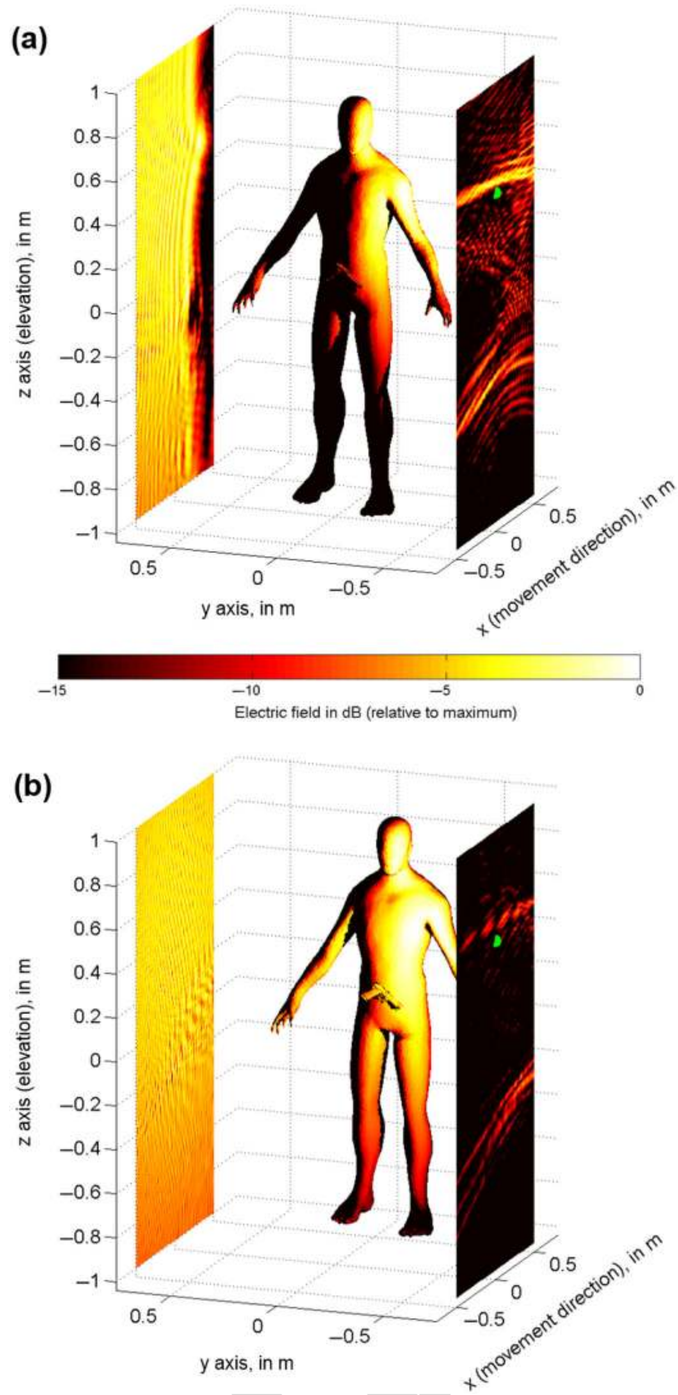

Fig. 14. Examples of human body illumination using one transmitter (highlighted in green) and scattered field on the array panels when the body model is centered in (a) 0.25 m and (b) 0.75 m.

areas of the body are illuminated. This layout increases the amount of information thanks to the spatial diversity of the multistatic illumination.

Regarding the inverse method to create images in this system and due to the large computational cost for the imaging, when the backpropagation is implemented in 3-D, the above-mentioned Fourier-based technique for multistatic imaging [9] has been used. The efficient use of fast Fourier transforms (FFT) provides 3-D whole body imaging in almost real time using conventional hardware.

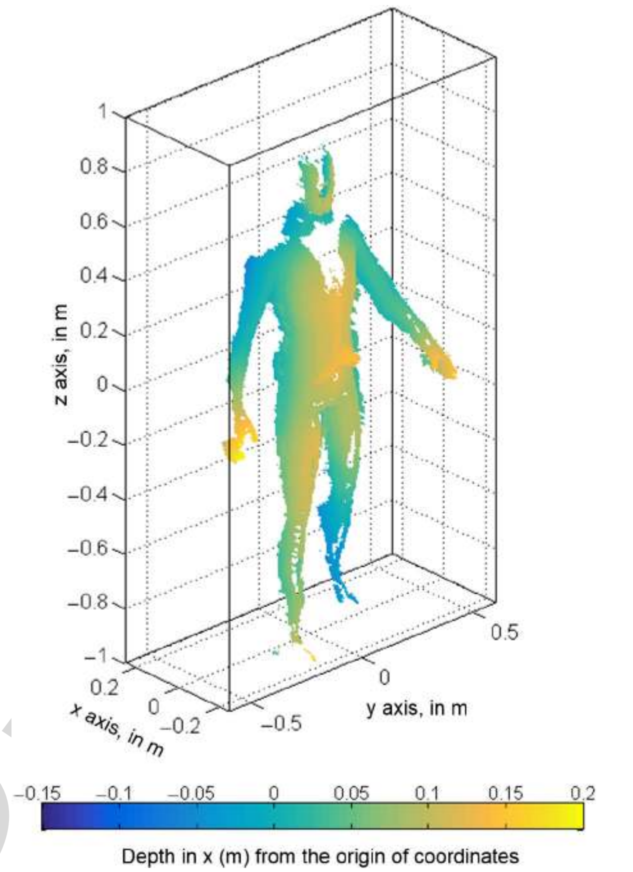

Fig. 15. Person placed at x = 0.25 m. Recovered human body and concealed object geometry from backpropagation imaging.

As an application example to show the performance of the proposed configuration, an OUT consisting on a person carrying a concealed weapon in the belt has been considered. For the sake of simplicity, only two positions are analyzed: person standing at x = 0.25 m and at x = 0.75 m. In this example, the goal is to clearly illustrate the different nature of the multistatic information collected on each position, rather than a rigorous reconstruction of the whole body.

For every position, transmitter, and receiving panel, the amount of data to be processed is: 201×401 spatial samples $\times$ 121 frequency samples ($= 9.75 \times 10^6$ scattered field samples), which also determines the number of imaging points in the case of Fourier-based imaging [9]. A workstation with 32 cores at 2.1 GHz and 128-GB RAM was used for data processing. Overall calculation time for every transmitter was 30 s (1200 s total for the 40 used transmitters). The processing has been done using a sequential Matlab code and has not been optimized for real time imaging yet.

Imaging results are depicted in Figs. 15 and 16, corresponding to the person's placement at x = 0.25 m and x = 0.75 m, respectively. Reflectivity points above -25 dB with respect to the maximum are coded in depth according to x-axis, allowing the recovery of the human body profile and potential concealed weapons. Comparison of Figs. 15 and 16 provides a clear example of the on-the-move imaging concept effectiveness. In the case of Fig. 15 (person placed at x = 0.25 m), the human body sides and some areas of the chest are imaged by the system. In

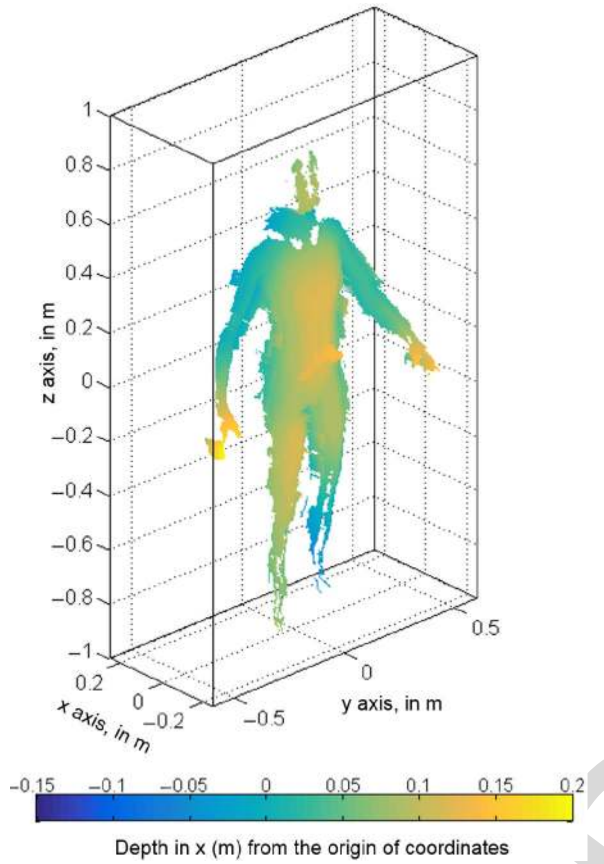

Fig. 16. Person placed at x = 0.75 m. Recovered human body and concealed object geometry from backpropagation imaging.

Fig. 16 (person placed at x = 0.75 m), the top of the chest and the shoulders are recovered.

In the final system, multiple images, as the two presented examples, can be created and analyzed at video rate to detect any possible threats. Algorithms for mesh generation and automatic thread detection, such as the one used in [8], can be applied.

VII. Conclusion

This work presented a novel concept for personnel scanning in airports and other checkpoints. Unlike the current imaging systems, the proposed system allows for continuous movement of the subject while being scanned; this will greatly increase the system throughput when compared with state-of-the-art systems. This improvement is possible thanks to the use of a fully multistatic radar configuration, where some of the transmitters and receivers are separated with a subtended angle relative to the person greater than 90 degrees to capture information from all possible wave incident angles. In this way, the system is able to create a complete contour reconstruction as the person moves inside the system. The use of a small number of transmitters allows for fast image creation as all the transmitters can be sequentially activated in a short amount of time. 2-D and 3-D simulation-based results confirm the good imaging capabilities of the proposed system; 2-D results have also been validated using measurements. Further work will be related with the setup optimization, including the use of sparse arrays and other techniques to reduce the number of receivers, and with experimental validation.

References

[1] IATA. *Checkpoint of the Future. Executive Summary* [Online]. Available: http://www.iata.org/whatwedo/security/Documents/cof-executive-summary.pdf, accessed on Mar. 16, 2015.

[2] S. S. Ahmed, A. Schiessl, F. Gumbmann, M. Tiebout, S. Methfessel, and L. Schmidt, "Advanced microwave imaging," *IEEE Microw. Mag.*, vol. 13, no. 6, pp. 26–43, Sep./Oct. 2012.

[3] S. S. Ahmed, "Personnel screening with advanced multistatic imaging technology," in *Proc. SPIE Defense Secur. Sens.*, 2013, p. 87150B.

[4] D. Sheen, D. McMakin, and T. Hall, "Three-dimensional millimeter-wave imaging for concealed weapon detection," *IEEE Trans. Microw. Theory Techn.*, vol. 49, no. 9, pp. 1581–1592, Sep. 2001.

[5] X. Zhuge and A. Yarovoy, "A sparse aperture MIMO-SAR-based UWB imaging system for concealed weapon detection," *IEEE Trans. Geosci. Remote Sens.*, vol. 49, no. 1, pp. 509–518, Jan. 2011.

[6] D. M. Sheen, D. L. McMakin, and T. E. Hall, "Combined illumination cylindrical millimeter-wave imaging technique for concealed weapon detection," in *Proc. AeroSense*, 2000, pp. 52–60.

[7] Y. Rodríguez-Vaqueiro, Y. Álvarez López, B. Gonzalez-Valdes, J. A. Martinez, F. Las-Heras, and C. M. Rappaport, "On the use of compressed sensing techniques for improving multistatic millimeter-wave portal-based personnel screening," *IEEE Trans. Antennas Propag.*, vol. 62, no. 1, pp. 494–499, Jan. 2014.

[8] B. Gonzalez-Valdes, Y. Alvarez-Lopez, J. A. Martinez-Lorenzo, F. Las Heras Andres, and C. M. Rappaport, "On the use of improved imaging techniques for the development of a multistatic three-dimensional millimeter-wave portal for personnel screening," *Prog. Electromagn. Res.*, vol. 138, pp. 83–98, 2013.

[9] Y. Alvarez *et al.*, "Fourier-based imaging for multistatic radar systems," *IEEE Trans. Microw. Theory Techn.*, vol. 62, no. 8, pp. 1798–1810, Aug. 2014.

[10] G. Yates, A. Horne, A. Blake, and R. Middleton, "Bistatic SAR image formation," *Inst. Elect. Eng. Proc. Radar Sonar Navigat.*, vol. 153, no. 3, pp. 208–213, Jun. 2006.

[11] R. Burkholder, I. Gupta, and J. Johnson, "Comparison of monostatic and bistatic radar images," *IEEE Trans. Antennas Propag. Mag.*, vol. 45, no. 3, pp. 41–50, Jun. 2003.

[12] B. Gonzalez-Valdes, C. Rappaport, and J. A. Lorenzo-Martinez, "On-the-move active millimeter wave interrogation system using a hallway of multiple transmitters and receivers," in *Proc. IEEE Antennas Propag. Soc. Int. Symp. (APSURSI)*, 2014, pp. 1107–1108.

[13] B. Gonzalez-Valdes, C. Rappaport, and J. Martinez-Lorenzo, "On the move millimiter wave interrogation system with a hallway of multiple transmitters and receivers," U.S. Patent 14 562 094, Dec. 5, 2014.

[14] M. Soumekh, "Bistatic synthetic aperture radar inversion with application in dynamic object imaging," *IEEE Trans. Signal Process.*, vol. 39, no. 9, pp. 2044–2055, Sep. 1991.

[15] Y. Alvarez, J. Martinez, F. Las-Heras, and C. Rappaport, "An inverse fast multipole method for imaging applications," *IEEE Antennas Wireless Propag. Lett.*, vol. 10, pp. 1259–1262, Nov. 2011.

[16] D. Andreuccetti, R. Fossi, and C. Petrucci, "An Internet resource for the calculation of the dielectric properties of body tissues in the frequency range 10 Hz–100 GHz," Internet document, 1997 [Online]. Available: http://niremf.ifac.cnr.it/tissprop/, accessed on Sep. 15, 2015, IFAC-CNR, Florence, Italy, 1997, based on data published by C. Gabriel et al. in 1996.

[17] A. W. Morgenthaler and C. M. Rappaport, "Scattering from lossy dielectric objects buried beneath randomly rough ground: Validating the semi-analytic mode matching algorithm with 2-D FDFD," *IEEE Trans. Geosci. Remote Sens.*, vol. 39, no. 11, pp. 2421–2428, Nov. 2001.

[18] C. M. Rappaport, Q. Dong, E. Bishop, A. Morgenthaler, and M. E. Kilmer, "Finite difference frequency domain (FDFD) modeling of two dimensional TE wave propagation," in *Proc. URSI Symp. Conf.*, Pisa, Italy, 2004.

[19] A. Arboleya, Y. Alvarez, and F. Las-Heras, "Millimeter and submillimeter planar measurement setup," in *Proc. IEEE Antennas Propag. Soc. Int. Symp. (APSURSI)*, 2013, pp. 1–2.

[20] S. S. Ahmed, A. Schiessl, and L.-P. Schmidt, "A novel active real-time digital-beamforming imager for personnel screening," in *Proc. 9th Eur. Conf. Synth. Aperture Radar (EUSAR)*, Apr. 2012, pp. 178–181.

[21] J. Meana, J. Martinez-Lorenzo, F. Las-Heras, and C. Rappaport, "Wave scattering by dielectric and lossy materials using the modified equivalent current approximation (MECA)," *IEEE Trans. Antennas Propag.*, vol. 58, no. 11, pp. 3757–3761, Nov. 2010.

[22] L. E. Tirado, J. A. Martinez-Lorenzo, B. Gonzalez-Valdes, C. Rappaport, O. Rubinos-Lopez, and H. Gomez-Sousa, "GPU implementation of the modified equivalent current approximation (MECA) method," *Appl. Comput. Electromagn. Soc. J.*, no. 9, Sep. 2012.

[23] J. Gutiérrez Meana, F. L. Las Heras Andrés, and J. Á. Martínez Lorenzo, "A comparison among fast visibility algorithms applied to computational electromagnetics," *Appl. Comput. Electromagn. Soc. J.*, 2009.

Borja Gonzalez-Valdes (M'xx) received the B.S and Ph.D. degrees in electrical engineering from the University of Vigo, Vigo, Spain, in 2006 and 2010, respectively.

From 2006 to 2010, he was with the Antenna and Optical Communications Group, University of Vigo. From 2008 to 2009, he was a Visiting Researcher with the Gordon Center for Subsurface Sensing & Imaging Systems, Northeastern University, Boston, MA, USA. In 2011, he joined the Awareness and Localization of Explosives-Related Threats Center of Excellence, Northeastern University. Since 2015, he has been a Postdoctoral Researcher affiliated with the AtlantTIC Research Center, University of Vigo. His research interests include antenna design, inverse scattering, radar, advanced imaging techniques, and THz technology.

Yuri Álvarez (S'06–M'09–SM'15) was born in Langreo, Spain, in 1983. He received the M.S. and Ph.D. degrees in telecommunication engineering from the University of Oviedo, Gijn, Spain, in 2006 and 2009, respectively.

He was a Visiting Scholar at the Department of Electrical Engineering and Computer Science, Syracuse University, Syracuse, NY, USA, in 2006 and 2008; a Visiting Postdoc at the Gordon Center for Subsurface Sensing and Imaging Systems (CenSSIS)ALERT (Awareness and Localization of Explosive Related Threats) Center of Excellence, Northeastern University, Boston, MA, USA, from 2011 to 2014; and a Visiting Postdoc at ELEDIA Research Center, Trento, Italy, in 2015. He is currently an Assistant Professor with the Signal Theory and Communications, University of Oviedo, Gijn, Spain. His research interests include antenna diagnostics, antenna measurement techniques, RF techniques for indoor location, inverse scattering and imaging techniques, and phaseless methods for antenna diagnostics and imaging.

Dr. Alvarez was the recipient of the 2011 Regional and National Awards to the Best Ph.D. Thesis on Telecommunication Engineering (category: security and defense).

Yolanda Rodriguez-Vaqueiro (S'xx) received the B.S. and M.S. degrees in electrical engineering from the University of Vigo, Vigo, Spain, in 2009, and the Ph.D. degree in electrical engineering from Northeastern University, Boston, MA, USA, in 2015 (after defending her thesis: Compressive Sensing for Electromagnetic Imaging Using a Nesterov-Based Algorithm).

She is a Postdoctoral Researcher affiliated with the AtlantTIC Research Center, University of Vigo. In 2011, she obtained a Research Assistant grant from the ALERT (Awareness and Localization of Explosive Related Threats) Center of Excellence, Northeastern University. She was also granted as a Junior Researcher with the University of Vigo.

Dr. Rodriguez-Vaqueiro was the recipient of the Research-Impact Award by the Department of Electrical and Computer Engineering, Northeastern University (for her work during the Ph.D. studies), the Best Paper Award in the 2012 IEEE Homeland Security Conference, Honorable Mention in the Student Paper Competition in the 2013 IEEE APS/URSI Conference, the Best Paper Award in the 2014 European Conference on Antennas and Propagation, the Burke/Yannas Award to the most original research study in the field of bioengineering in the 2015 American Burn Association (ABA) Meeting, and the Research-Impact Award by the Department of Electrical and Computer Engineering, Northeastern University, in May 2015.

Ana Arboleya-Arboleya received the M.Sc. degree in telecommunication engineering from the University of Oviedo, Oviedo, Spain, in 2009, where she is currently pursuing the Ph.D. degree in telecommunication engineering. Since 2008, she has been a Research Assistant within the Signal Theory and Communications Research Group, TSC-UNIOVI, Department of Electrical Engineering, University of Oviedo. She was a Visiting Scholar in 2014 and 2015 at the Department of Radio Science and Engineering and MilliLab, Aalto University, Espoo, Finland. Her research interests include antenna diagnostics and measurement systems and techniques and high-frequency imaging techniques and applications.

Antonio García-Pino (S'87–M'89–SM'05) was born in Valdemoro, Madrid, Spain, in 1962. He received the M.S. and Ph.D. degrees in telecommunications engineering from the Polytechnic University of Madrid (UPM), Madrid, Spain, in 1985 and 1989, respectively.

From 1985 to 1989, he was a Research Assistant with the Radiation Group, UPM. He joined as an Associate Professor with the Department of Technologies of Communications, University of Vigo, Vigo, Spain, in 1989, becoming Full Professor in 1994. In 1993, he was a Visiting Researcher at the Center for Electromagnetics Research, Northeastem University, Boston, MA, USA. From 2006 to 2010, he was the Vice-Rector of Academic Organization and Faculty, and currently, he is the Director of the International Doctoral School, both at University of Vigo. His research interests include shaped-reflector antennas for communication and radar applications, high-frequency backscattering, computational electromagnetics, and THz technology. In these topics, he has authored more than 100 technical papers in journal and conferences and he has been an advisor of 14 Ph.D. thesis.

Carey M. Rappaport (SM'96–F'06) received the S.B. degree in mathematics, the S.B., S.M., and E.E. degrees in electrical engineering in 1982, and the Ph.D. degree in electrical engineering in 1987 from the Massachusetts Institute of Technology (MIT), Cambridge, MA, USA.

He was a Teaching and Research Assistant with MIT from 1981 until 1987, and during the summers at COMSAT Labs, Clarksburg, MD, USA, and the Aerospace Corp., El Segundo, CA, USA. He joined the faculty at Northeastern University, Boston, MA, USA, in 1987. He has been a Professor of Electrical and Computer Engineering since July 2000. In 2011, he was appointed as a College of Engineering Distinguished Professor. In fall 1995, he was a Visiting Professor of Electrical Engineering at the Electromagnetics Institute, Technical University of Denmark, Lyngby, Denmark, as part of the W. Fulbright International Scholar Program. In the second half of 2005, he was a Visiting Research Scientist at the Commonwealth Scientific Industrial and Research Organisation (CSIRO), Epping, Australia. He has consulted for CACI, Alion Science and Technology, Inc., Geo-Centers, Inc., PPG, Inc., and several municipalities on wave propagation and modeling, and microwave heating and safety. He was the Principal Investigator of an ARO-sponsored Multidisciplinary University Research Initiative on Humanitarian Demining, the Co-Principal Investigator of the NSF-sponsored Engineering Research Center for Subsurface Sensing and Imaging Systems (CenSSIS), and the Co-Principal Investigator and Deputy Director of the DHS-sponsored Awareness and Localization of Explosive Related Threats (ALERT) Center of Excellence. He has authored more than 400 technical journal and conference papers in the areas of microwave antenna design, electromagnetic wave propagation and scattering computation, and bioelectromagnetics, and has received two reflector antenna patents, two biomedical device patents, and four subsurface sensing device patents.

Prof. Rappaport is a member of Sigma Xi and Eta Kappa Nu professional honorary societies. He was the recipient of the IEEE Antenna and Propagation Society's H. A. Wheeler Award for the Best Applications Paper, as a Student in 1986.

Fernando Las-Heras (M'86–SM'08) received the M.S. and Ph.D. degrees in telecommunication engineering from the Technical University of Madrid (UPM), Madrid, Spain, in 1987 and 1990, respectively.

He was a National Graduate Research Fellow (1988–1990), and he held a position of Associate Professor with the Department of Signal, Systems, and Radiocommunications, UPM (1991–2000). From December 2003, he holds a Full Professor position with the University of Oviedo, Oviedo, Spain, where he was the Vice-Dean for Telecommunication Engineering, Technical School of Engineering, Gijón, Spain (2004–2008). As of 2001, he was the Head of the Research Group Signal Theory and Communications TSC-UNIOVI, Department of Electrical Engineering, University of Oviedo. He was a Visiting Lecturer at the National University of Engineering, Rímac Lima, Peru, in 1996, a Visiting Researcher at Syracuse University, Syracuse, NY, USA, in 2000, and a short-term Visiting Lecturer at ESIGELEC, France, from 2005 to 2011. He held the Telefónica Chair on RF Technologies, ICTs applied to Environment and ICTs and Smartcities with the University of Oviedo (2005–2015). He has authored more than 300 articles published in academic journals and proceedings of international conferences, mainly in the areas of antenna design and the inverse electromagnetic problem with applications in diagnostic, measurement and synthesis of antennas, phaseless techniques, propagation, and microwave to THz imaging and localization, as well as in engineering education.

Dr. Las-Heras was a Member of the Board of Directors of the IEEE Spain Section (2012–2015), and from 2010, he was a Member of the Science, Technology, and Innovation Council of Asturias, Asturias, Spain.

Jose A. Martinez-Lorenzo (M'xx) received the B.S./M.S. degree in 2002 and the Ph.D. degree in 2005 from the University of Vigo, Vigo, Spain, both in electrical engineering.

He joined the faculty at University of Oviedo, Gijon, Spain, in 2004, where he was an Assistant Professor with the Department of Signal Theory and Communications. In 2006, he joined Bernard M. Gordon Center for Subsurface Sensing and Imaging Systems, Northeastern University, Boston, MA, USA. In 2010, he was a Research Assistant Professor with the Department of ECE, Northeastern University. Since August 2013, he has been held a joint appointment with the Departments of MIE and ECE as a Tenure-Track Assistant Professor. He is an Active Member of Awareness and Localization of Explosives-Related Threats (ALERT) a DHS Center of Excellence awarded to Northeastern University. He has authored more than 140 technical journal and conference papers. His research interests include the understanding, modeling, and solving complex engineering problems, with an emphasis on mechanical and electromagnetic sensing and imaging methods for security and biomedical applications (i.e., explosive detection, breast cancer detection).

Prof. Martinez-Lorenzo has received funding from multiple agencies, including: DHS, DARPA, NSF, US Army, and the European Space Agency (ESA). He led the team that won the Best Paper Award in the 2012 IEEE Conference on Technologies for Homeland Security, for the paper on a compressed sensing approach for detection of explosive threats at standoff distances using a passive array of scatterers.

QUERIES

Q1: Please provide captions for Fig. 3 subparts.

Q2: Please provide year of publication for Ref. [1].

Q3: Please provide page range for Refs. [18], [22], and [23].

Q4: Please provide volume number for Ref. [22] and [23].

Q5: Please provide the membership history (year) of the authors Borja Gonzalez-Valdes, Yolanda Rodriguez-Vaqueiro,and Jose A. Martinez-Lorenzo.

Q6: Please provide year of completion for the S.B. degree in Mathematics, S.B., S.M. degrees in electrical engineering of author "Carey M. Rappaport."

Millimeter Wave Imaging Architecture for On-The-Move Whole Body Imaging

Borja Gonzalez-Valdes, *Member, IEEE*, Yuri Álvarez, *Senior Member, IEEE*, Yolanda Rodriguez-Vaqueiro, *Student Member, IEEE*, Ana Arboleya-Arboleya, Antonio García-Pino, *Senior Member, IEEE*, Carey M. Rappaport, *Fellow, IEEE*, Fernando Las-Heras, *Senior Member, IEEE*, and Jose A. Martinez-Lorenzo, *Member, IEEE*

***Abstract*—This paper presents a novel interrogation system that combines multiple millimeter wave transmitters and receivers to create real-time high-resolution radar images for personnel security screening. The main novelty of the presented system is that the images can be created as the person being screened continuously moves across a corridor where the transmitters and receivers, working in a fully coherent architecture, are distributed. As the person moves, the transmitters and receivers are sequentially activated to collect data from different angles to inspect the whole body. Multiple images, similar to video frames, are created and examined to look for possible anomalies such as concealed threats. Two-dimensional (2-D) and three-dimensional (3-D) setups have been simulated to show the feasibility of the proposed system. The simulation results in 2-D have been validated using measurements.**

***Index Terms*—Backpropagation imaging, checkpoint, fast Fourier transform (FFT), imaging systems, multistatic radar system.**

I. Introduction

In homeland security applications, there is an increasing demand for methods to improve personnel screening for concealed object and contraband detection at security checkpoints. In this context, active nearfield millimeter-wave (mm-wave) imaging radar systems are able to provide high-resolution imaging at an affordable cost. The object of interest is first illuminated by mm waves and then the scattered field is measured and processed to reconstruct the surface (or volume) of the object.

The development of checkpoints that allow high passenger flow is becoming a priority. This has motivated the design of mm-wave imaging systems that minimize passenger inconvenience.

The International Air Transport Association (IATA) has defined several specifications that future checkpoints for personnel screening should meet. Novel paradigms in the design of the checkpoints specify that "from 2020 and beyond it is envisaged that the passenger will be able to flow through the security checkpoint without interruption unless the advanced technology identifies a potential threat," [1] (page 14).

In [1], a computer graphics design of the checkpoint of the future proposed by IATA is presented. The novelty with respect to existing architectures is the inclusion of a beltway or hallway to avoid passenger flow interruption.

Current state-of-the-art mm-wave imaging systems for security screening require people to enter and stand in front of the scanning system. Mm-wave generation and acquisition can be achieved using static arrays of transmitters and receivers [2], [3], or using movable arrays to create planar [4], [5], or cylindrical [6]–[8] acquisition domains. Most of them are based on monostatic radar and Fourier inversion [2]–[6]. Monostatic imaging systems are cost effective, but they are only able to reconstruct surfaces that create specular reflection and they are not well suited for imaging scattering objects with sudden profile variations [9]. Further, they are prone to dihedral artifacts as described in [8], [10], and [11].

Based on the new checkpoint architecture proposed by the IATA, this paper introduces a novel concept for mm-wave scanning system for personnel screening. The proposed imaging system does not include any mechanical movement, and whole body imaging is obtained taking advantage of the movement of the person under test when passing through the system on a moving walkway.

The main contribution of this paper is the introduction of this novel architecture, called on-the-move imaging [12], [13], that, to the best of the author's knowledge, has not been previously conceived nor demonstrated.

This paper is structured as follows. Section II describes the proposed mm-wave screening system. Imaging algorithm for multistatic setups is briefly described in Section III. Proof-of-concept is validated through two-dimensional (2-D) simulation

Manuscript received June 18, 2015; revised January 11, 2016; accepted February 18, 2016. Date of publication XXXX XX, XXXX; date of current version XXXX XX, XXXX. This work was supported in part by the Ministerio de Ciencia e Innovacin of Spain/FEDER under project MIRIIEM-TEC2014-54005-P, in part by the Gobierno del Principado de Asturias through the PCTI 2013-2017, GRUPIN14-114, in part by the Spanish Government under project TACTICA, in part by the European Regional Development Fund (ERDF), in part by the Galician Regional Government under Projects CN2012/279, CN2012/260 (AtlantTIC) and the Plan I2C (2011–2015), and in part by the Science and Technology Directorate, U.S. Department of Homeland Security under the Award Number 2008-ST-061-ED0001.

B. Gonzalez-Valdes, Y. Rodriguez-Vaqueiro, and A. García-Pino are with the Atlantic Research Center, Universidad de Vigo, 36310 Vigo, Spain (e-mail: bgvaldes@com.uvigo.es; yrvaqueiro@com.uvigo.es; agpino@com.uvigo.es).

Y. Álvarez, A. Arboleya Arboleya, and F. Las-Heras are with the Area of Signal Theory and Communications, Department of Electrical Engineering, Universidad de Oviedo, E-33203 Gijón, Spain (e-mail: yalopez@tsc.uniovi.es; aarboleya@tsc.uniovi.es; flasheras@tsc.uniovi.es).

C. M. Rappaport and J. A. Martinez are with the ALERT Center, Northeastern University, Boston, MA 02115 USA (e-mail: rappapor@ece.neu.edu; jmartine@ece.neu.edu).

Color versions of one or more of the figures in this paper are available online at http://ieeexplore.ieee.org.

Digital Object Identifier 10.1109/TAP.2016.2539372

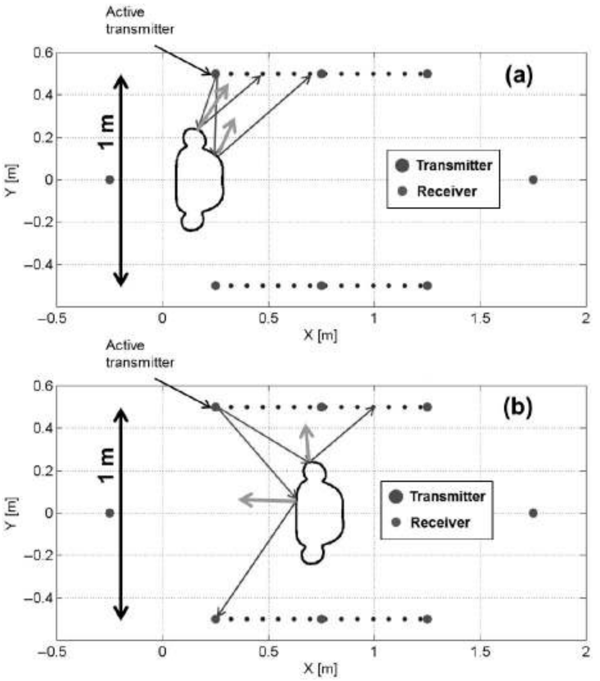

Fig. 1. On-the-move imaging concept. OUT movement between the two walls of radar antennas provides multiple points-of-view for every transmitter and receiver, thus increasing multistatic information. (a) and (b) represent two different OUT positions within the hallway.

examples in Section IV, and measurement results in Section V. Extension to two-dimensional (3-D) whole human body imaging is described and validated in Section VI. Finally, the conclusion is presented in Section VII.

II. On-the-Move Hallway Concept

The novel mm-wave on-the-move imaging system for personnel screening takes advantage of: 1) the movement of the person when passing through the imaging system and 2) a multistatic radar configuration, where some of the transmitters and receivers are separated with a subtended angle relative to the person equal or greater than 90° to capture information from all possible wave incident and scattering angles.

A top view of the suggested multistatic architecture is plotted in Fig. 1. Several transmitters (red dots) and receivers (blue dots) are placed on the sides of the hallway. The person moves along the security checkpoint on a moving walkway.

The imaging radar system takes advantage of multiple incidence angles that illuminate different areas of the person depending on the active transmitter and the placement of the person within the hallway, as illustrated in Fig. 1. A single transmitter can illuminate different areas of the person while crossing the hallway. Reciprocally, the scattered field is collected by different receivers depending on the transmitting element and the current position of the person. This is illustrated with the red and blue arrows in Fig. 1 that represent direct reflection contributions given by the incident angle and the normal to the surface according to Snell's law.

Multistatic information can be incremented by placing transmitters at the hallway ends. For practical implementation, this

TABLE I
Comparison With State-of-the-Art mm-Wave Imaging Systems

Reference	Scanning area (cm)[1]	PSF (mm)[2]	Frequency band (GHz)	Number of antennas
On-the-move	100×200[3]	10×10	15 – 30	2×80601 Rx 60 Tx
UWB MIMO array, [5]	50×130	10×10	2.8 – 19.5	4 Tx 8 Rx, Height motion.
Flat 2-D array, [2]	100×200	3.0×1.5	72 – 80	3072 Tx 3072 Rx
Linear array, vertical movement [4]	72.6 Movable 2 m in height	10.0×3.8	27 – 33	66 Tx, 66 Rx, Height motion

[1]Scanning area size: width ×height.
[2]PSF (point spread function): range ×cross range.
[3]Receiving panels size.

would partially block the persons path. This is solved in the 3-D case placing the receivers at the hallway ends below and above the moving walkway.

For every transmitter, the scattered field is collected on the receiving arrays placed on the hallway sides, and for every receiving array, a reflectivity image is recovered. The reflectivity images associated with each transmitter are coherently combined. This configuration assumes that, for a single position, the body remains still while all the transmitters are sequentially activated and the scattered field is collected by the receivers. In this sense, and since the acquisition on the receivers can be done in parallel, the use of a low number of transmitters is desirable. A fully electronic scanning system similar to the one in [3] would easily allow for such an acquisition procedure.

A critical aspect in the design of the imaging system is the selection of the frequency band. Table I shows a comparison among the proposed hallway concept and some of the existing mm-wave scanning systems. It can be observed that, for a given size of the scanner, higher frequency bands provide better cross-range resolution, at the expense of losing dynamic range due to free-space propagation losses. Furthermore, clothing becomes less transparent for these higher frequency bands, and radiofrequency hardware becomes more expensive. The work presented in [5] addresses the aforementioned drawbacks introducing an ultra-wideband (UWB) imaging system. In addition to the improved range resolution and dynamic range, the novelty of this study is the fact that the sampling rate can be relaxed by taking advantage of grating lobes cancellation in UWB arrays, which will be of interest concerning practical implementation of the on-the-move architecture.

III. Imaging Algorithm

Practical mm-wave scanning system implementation demands real-time imaging capabilities. Standard backpropagation techniques [14] require millions of calculations for electrically large acquisition and imaging domains. To illustrate the numerical magnitude of the problem, typical values for acquisition points and imaging voxels are 10^5 and 10^7, respectively, assuming an operational frequency of 30 GHz ($\lambda = 1$ cm) and sampling every half wavelength in both domains according to Nyquist criterion.

The reflectivity function on a volumetric domain $\rho_t(x', y', z')$ can be recovered from the scattered field $E^t_{scatt}(f, x, z)$ acquired on a flat receiving aperture placed at $y = Y_0$, by solving the following integral equation [9], [14], when the *t*th (with *t* from 1 to N_{tx}) of a group of transmitters is active

$$\rho_t(x', y', z') = \iiint E^t_{scatt}(f, x, z) e^{+jk((x-x')^2+(Y_0-y')^2+(z-z')^2)^{1/2}} e^{+jk((x^t_{inc}-x')^2+(y^t_{inc}-y')^2+(z^t_{inc}-z')^2)^{1/2}} df dx dz \quad (1)$$

where $(x^t_{inc}, y^t_{inc}, z^t_{inc})$ denotes the position of the tth point source-like transmitter, $k = 2\pi f/c$, y-axis is the range axis (depth), x- and z-axes are horizontal and vertical cross ranges, and f is the frequency.

Fast propagation techniques, such as the inverse fast multipole method, have been proposed [15], reducing the calculation time by several orders of magnitude. Moreover, (1) can be parallelized taking advantage of GPU hardware. However, these solutions are still too computationally expensive for applications requiring real-time imaging.

Fourier-based techniques have been widely used in monostatic setups for real-time imaging [3]–[5], thanks to the fact that plane wave incidence can be considered during the inversion. Multistatic setups require different Fourier processing as the transmitter and receiver are placed in different positions. A novel Fourier-based imaging technique, totally suitable for the proposed hallway-based on-the-move imaging system, is presented in [9]. The idea is to decompose the imaging domain in smaller regions where an incident spherical wave can be locally treated as a plane wave. Imaging calculations for every region can be carried out in parallel, without jeopardizing the required real-time capabilities of the multistatic imaging system.

When multiple transmitters are used, the final reconstruction for a certain voxel placed in (x', y', z') can be obtained by combining the images generated by each transmitter as

$$\rho(x', y', z') = \sum_{t=1}^{N_{tx}} \rho_t(x', y', z'). \quad (2)$$

This formulation assumes all the transmitters and receivers work in a fully coherent configuration using a clock signal that provides common phase reference.

IV. 2-D Results

The proposed on-the-move imaging is first validated using a 2-D example. The frequency band ranges from 15 to 30 GHz, sampled every 300-MHz frequency steps and providing 1-cm range resolution. Two 1-m width lateral arrays of receivers with 50 evenly spaced elements are placed at $Y_0 = -0.6$ m and $Y_0 = 0.6$ m . Five transmitters are interleaved among each

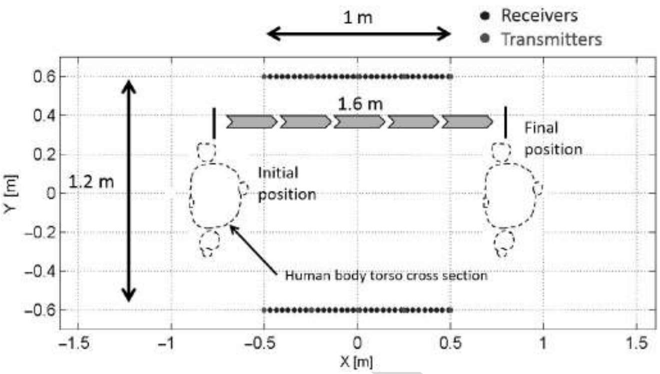

Fig. 2. 2-D example layout. OUT is displaced from position $x = -0.8$ m to $x = +0.8$ m, in five steps ($N_{pos} = 5$). 5 Tx and 50 Rx per side are considered.

panel of receivers, thus resulting in $N_{tx} = 10$ transmitters. The described layout is plotted in Fig. 2. The essential aspect is that, in order to image the entire body surface, for every transmitter, receivers on both walls must receive the scattered waves (not just those adjacent to a given transmitter.)

The object under test (OUT) models the cross section of a human body torso (for a more realistic simulation, arms, and waist are not connected), with three attached objects on it represented as protrusions on the front, back, and arm. The object in the front is an elliptical cross-sectional metallic object. Dielectric objects ($\epsilon_r = 3.5$) are placed on the back (square cross section) and on the right arm. The OUT is displaced from the position $x = -0.8$ m to $x = 0.8$ m in 40-cm steps obtaining $N_{pos} = 5$ intermediate positions. For every position, the ten transmitters are sequentially activated and the scattered field is collected in the receiving points. A realistic composition of the human body tissue is considered [16], using a finite-difference frequency-domain (FDFD) code [17], [18] to calculate the scattered field for every transmitter and every OUT position. FDFD simulation results have confirmed that, due to the high conductivity of the skin in the frequency band of interest, the assumption that the OUT is a perfect electric conductor (PEC) is a good approximation for most cases.

The data are then used to create one reflectivity image for each intermediate position, ρ^p according to (1) and (2). The imaging domain is an $(X, Y) = (0.4, 0.6)$m rectangle, discretized in 81×121 pixels and centered in (x'_p, y'_p, z'_p). In this case, the computational cost is low and the image is recovered using the standard backprogation algorithm in (1). For every pth OUT position and tth active transmitter, the image is recovered in about 1 s using a conventional laptop (2.5-GHZ CPU and 4-GB RAM memory). As the 2-D imaging code is not parallelized yet, it takes about 50 s for the entire reconstruction.

The obtained images for two different active transmitters when the OUT is in each of the intermediate positions are presented in Fig. 3. It is clear that each transmitter allows the reconstruction of different areas of the body depending on its relative position inside the imaging system. The image obtained for the central position, combining the images created using all the transmitters according to (2), is presented in Fig. 4.

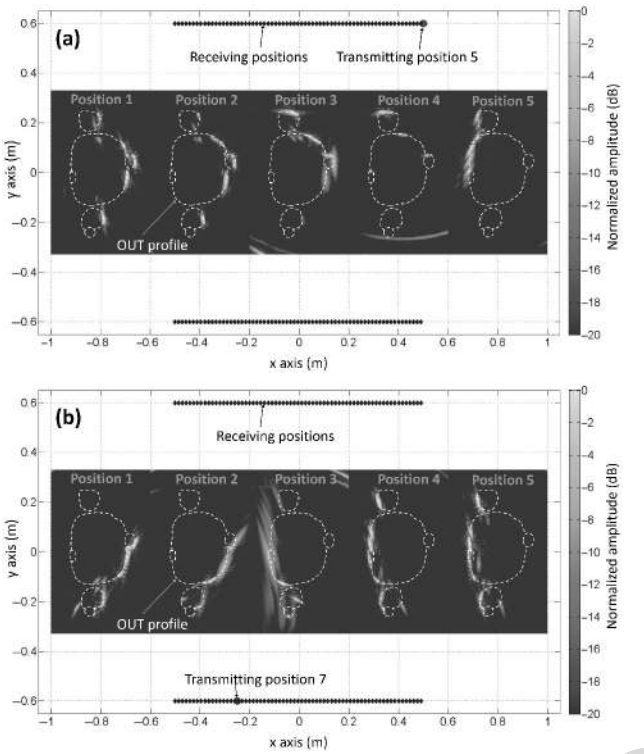

Fig. 3. Obtained images (normalized reflectivity amplitude in dB) for two different active transmitters and five intermediate positions using the setup in Fig. 2. Active transmitters are depicted as red points. Blue points represent receivers positions.

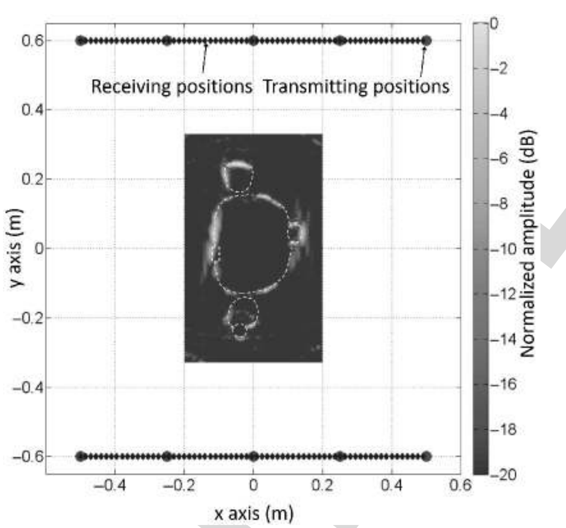

Fig. 4. Obtained image when the OUT is in the central position and the image is created using all transmitters according to (2).

The reflectivity image created by the system at each position is obtained as

$$I(x'', y'', z'') = \sum_{p=1}^{N_{pos}} |\rho(x' - x'_p, y' - y'_p, z' - z'_p)| \quad (3)$$

where the reflectivity of all the positions is centered at the origin of coordinates before being combined. Absolute value is used since the position of the OUT relative to the imaging system can slightly change from position to position, which prevents the combination of the images of each position in amplitude and phase. Fig. 5 presents the final result when the five analyzed positions are combined according to (3), and when the object retains exactly the same configuration for all positions and it is only displaced in the x direction. This proves the ability of the proposed system to obtain a complete contour reconstruction. In general, the images used for threat detection in a final configuration would be the ones generated in each position as the one in Fig. 4.

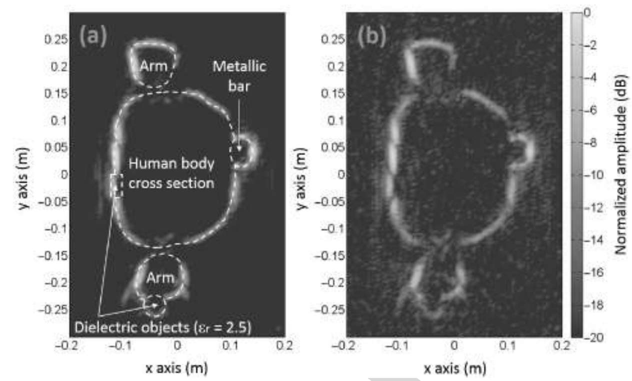

Fig. 5. Recovered OUT profile when combining in amplitude the five images (one for each position). (a) SNR = 10 dB. (b) SNR $= -20$ dB.

Combining the information from multiple transmitters and positions also helps to increase the dynamic range of the system. Sensitivity analysis has been performed: first, the recorded signal strength in the receiving arrays for every transmitting element and OUT position has been evaluated. The case in which maximum power is recorded corresponds to the OUT at the central position illuminated by the center transmitters. The minimum power levels are recorded for the OUT in positions 1 or 5 illuminated by the closest pair of transmitters, as only a small fraction of the scattered field is collected by the arrays. The received power difference between these two cases is 11 dB.

Next, noise has been added to the field samples according to different signal-to-noise ratio (SNR) levels relative to the maximum-recorded power case. Figs. 3–5(a) correspond to SNR = 10 dB, and Fig. 5(b) to SNR $= -20$ dB. Thanks to the combination of multiple OUT positions and incident directions, the resulting mm-wave imaging system is able to work with low SNR.

The capability of imaging multiple users within the hallway has been also evaluated. For this purpose, the OUT placed at the center position (as in Fig. 4) is considered, but with two more OUTs (with no attached objects) at $x = 0.7$ and $x - 0.7$ m, a scenario that could correspond to a high passenger throughput situation. Due to the use of FDFD simulations, multiple reflections among OUTs are considered. Results are depicted in Fig. 6. It can be noticed that, with respect to Fig. 4, the center OUT is worse imaged due to the multipath effects. It it also possible to create the image of the front and the back of the OUTs placed at $x = 0.7$ and $x = -0.7$ m, and these results are not affected by multipath as much as the center OUT.

In order to compare this work with current state of the art systems, Fig. 7 presents the obtained image when the same contour is facing a line containing the transmitters and receivers. In

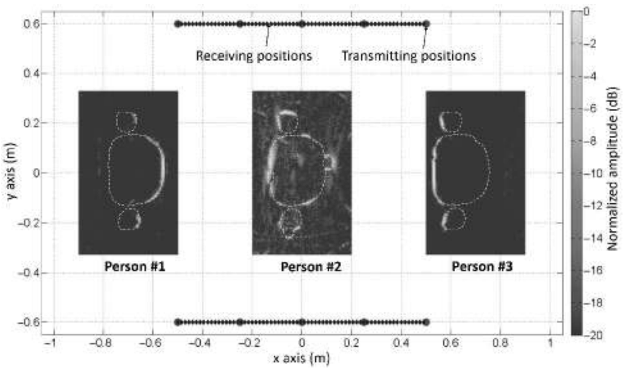

Fig. 6. Recovered image for three OUTs placed at the same time in the hallway. The image is created by combining all transmitters according to (2).

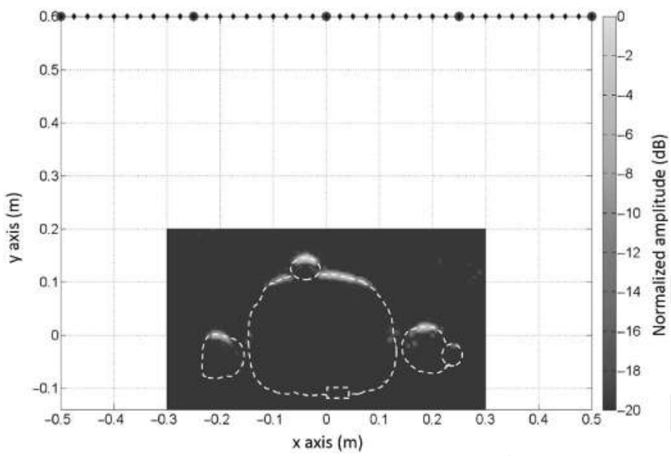

Fig. 7. Obtained image using state-of-the-art configurations where transmitters and receivers are placed in the same aperture and facing the person under test. The image is generated combining the five transmitters according (2).

this case, different areas of the front of the contour cannot be recovered and the area that is reconstructed is much smaller than the one of Fig. 4. Concerning detection capabilities, note that the dielectric object placed on the arm is hardly detected in Fig. 7 as the energy is not scattered back to the receiving array. In the case of the on-the-move system, it can be better detected (see Figs. 4 and 5), as it is possible to find a configuration along the conveyor belt in which the energy is reflected in the dielectric-skin transition, then backscattered to one of the receiving arrays.

This 2-D example proves that, in the proposed on-the-move layout, the fact that some of the transmitters and receivers are separated with a subtended angle relative to the person equal or greater than 90° provides information from all possible wave incident angles.

V. Validation With Measurements

The proposed on-the-move imaging concept has been validated with measurements. Ka frequency band (26.5–40 GHz) has been selected to avoid hardware switching between different frequency bands. In order to ensure the maximum illumination within the hallway, WR-28 open-ended waveguides are selected as antennas.

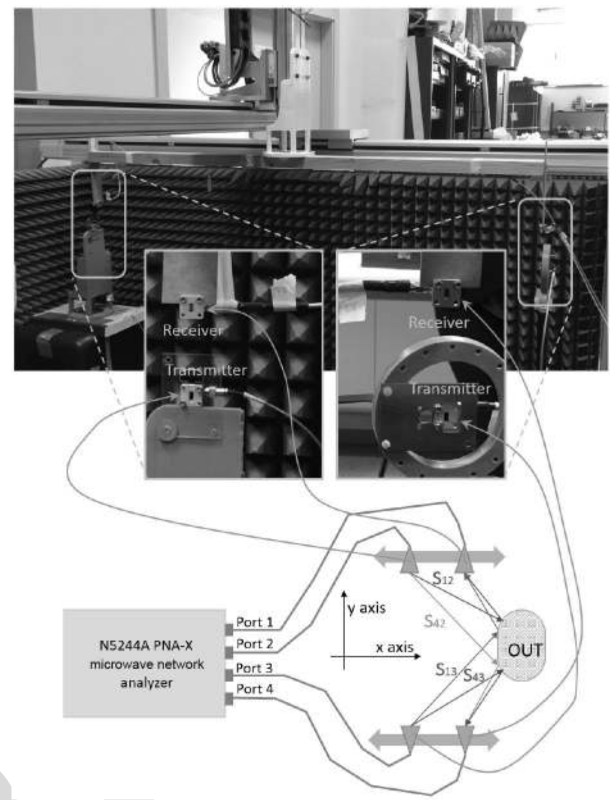

Fig. 8. Ka-band measurement system for on-the-move concept experimental validation. WR-28 open-ended waveguides are connected to the vector network analyzer ports. Receivers are mounted on a three-axis positioner.

The setup is mounted on an XYZ table measurement range [19], so some mechanical restrictions apply to the placement of the OUT, transmitters, and receiving positions (Fig. 8). In order to take advantage of the whole span of the XYZ measurement range, scattered field samples are collected in 161 points ranging from $x = -0.6$ m to $x = 0.6$ m, placed at $Y_0 = 0$ m and $Y_0 = 1.3$ m . Five transmitting positions are interleaved among the receivers, thus resulting in $N_{tx} = 10$ transmitting positions. Transmitters and receivers are separated 5 cm in height. Horizontal polarization is considered to reduce coupling between transmitter and receiver. The imaging setup is depicted in Fig. 8: two transmitters and two receivers are connected to the ports of a vector network analyzer. The power reference level is 0 dBm for all the ports. For every receiving position along the x-axis, four S-parameters are measured, as shown in Fig. 8, corresponding to the combination of each transmitter with both receivers.

The positioner of the XYZ table is used to move the receivers from each side of the hallway at the same time, as shown in Fig. 8. The pair of transmitters is manually placed at five positions along the x-axis, using the XYZ positioner as reference. For every pair of transmitting positions, acquisition time takes 3 min, and therefore, overall acquisition time for every OUT position is 15 min.

The OUT, shown in Fig. 9, is an aluminum foil-covered plastic bin with a metallic bar attached to one of the sides. Due to its translation symmetry in z-axis, it allows for 2-D analysis in an XY plane placed at $(z = h_{tx} + h_{rx}/2)$, where h_{tx} is the

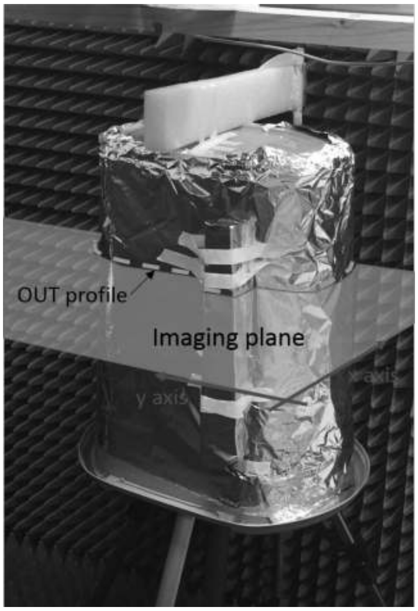

Fig. 9. Photograph of the OUT imaged with the proposed experimental setup. Receivers are mounted on a three-axis positioner.

height of the transmitters, and h_{rx} the height of the receivers. As mentioned in Section II, using metal to simulate the human body skin in the Ka band is an acceptable approach due to the high conductivity of the skin in mm-wave frequency bands [16]. Three positions of the OUT were considered.

The same data processing as in Section III has been applied. The image obtained for every position, combining the images created using all the transmitters according to (2), is depicted in Fig. 10(a). It can be noticed that, for positions 1 and 3, the front and the back of the OUT are imaged, and the sides of the OUT are visible for position 2.

Fig. 10(b) presents the final result combining the three OUT positions according to (3), where the OUT profile can be observed. In this case, combination is done taking the displacement of each individual image with respect to the center of the imaging domain. In practical, combination of the radar images for different positions of the person in the hallway can be based on video frames, linking video, and radar images.

In addition to the presented results, the measurement setup has been simulated, aiming to evaluate the correspondence between simulations and measurements. Results for position 2 are compared in Fig. 11. Good agreement between the reconstructed parts of the OUT for simulations and measurements is obtained.

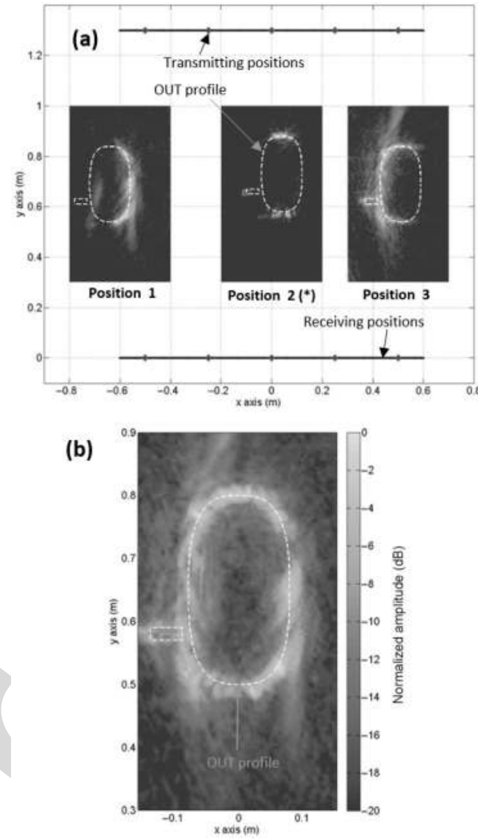

Fig. 10. Recovered OUT profile. (a) Image created on every position using all the transmitters according to (2). In the case of position 2, only the center transmitting positions ($x_{inc}^{t} = 0$ m) were available. (b) OUT profile when combining in amplitude the three images of (a).

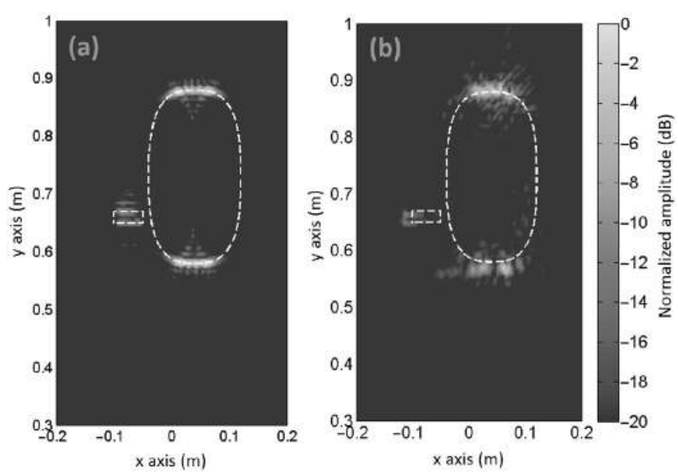

Fig. 11. Recovered OUT profile, position 2 (with center transmitting positions). (a) From simulated data. (b) From measurements.

VI. 3-D Configuration

Next, the extension from 2-D to 3-D is presented. The layout of the proposed on-the-move 3-D system is presented in Fig. 12. The setup is composed of multiple synchronized transmitters and receivers. Lateral receiving apertures of size (X, Z) = (1, 2) m, are placed at $Y_0 = 0.75$ m. The size of the panels is chosen to provide an approximated cross-range resolution of 1 cm along the z-axis and 2 cm in the x-axis.

For this preliminary setup, Nyquist sampling requirements are considered for the receiving panels, thus acquiring the field in 201×401 receiving positions per panel. Subsampling techniques as presented in [2] and [5] combined with a modified FFT algorithm for multistatic imaging with subsampled arrays can be efficiently applied in this setup to reduce the number of receivers in more than 90% [2], although this analysis is beyond the scope of this contribution. A 15-GHz bandwidth

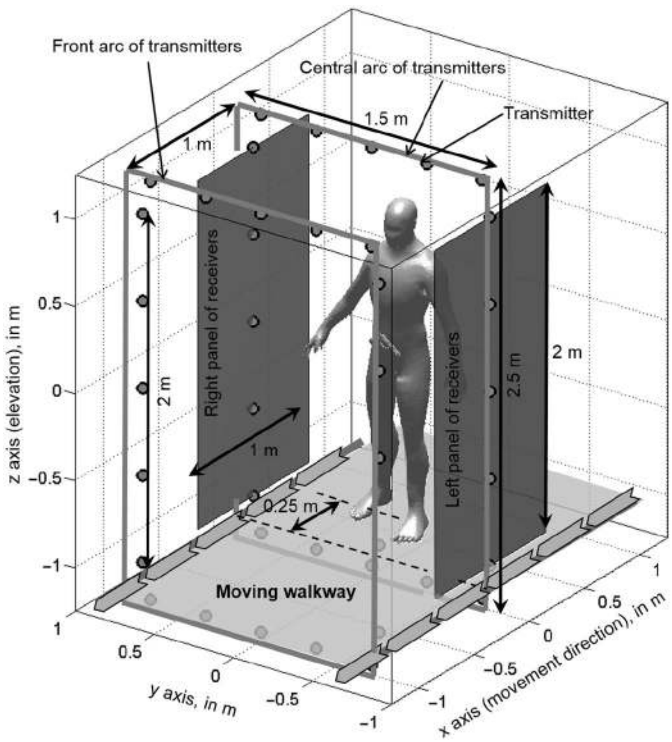

Fig. 12. Layout of the mm-wave scanner for personnel screening. For the sake of simplicity, just two arcs of transmitters, at x = 0 m, and x = −1 m, are considered. The person under test is placed at x = 0.25 m.

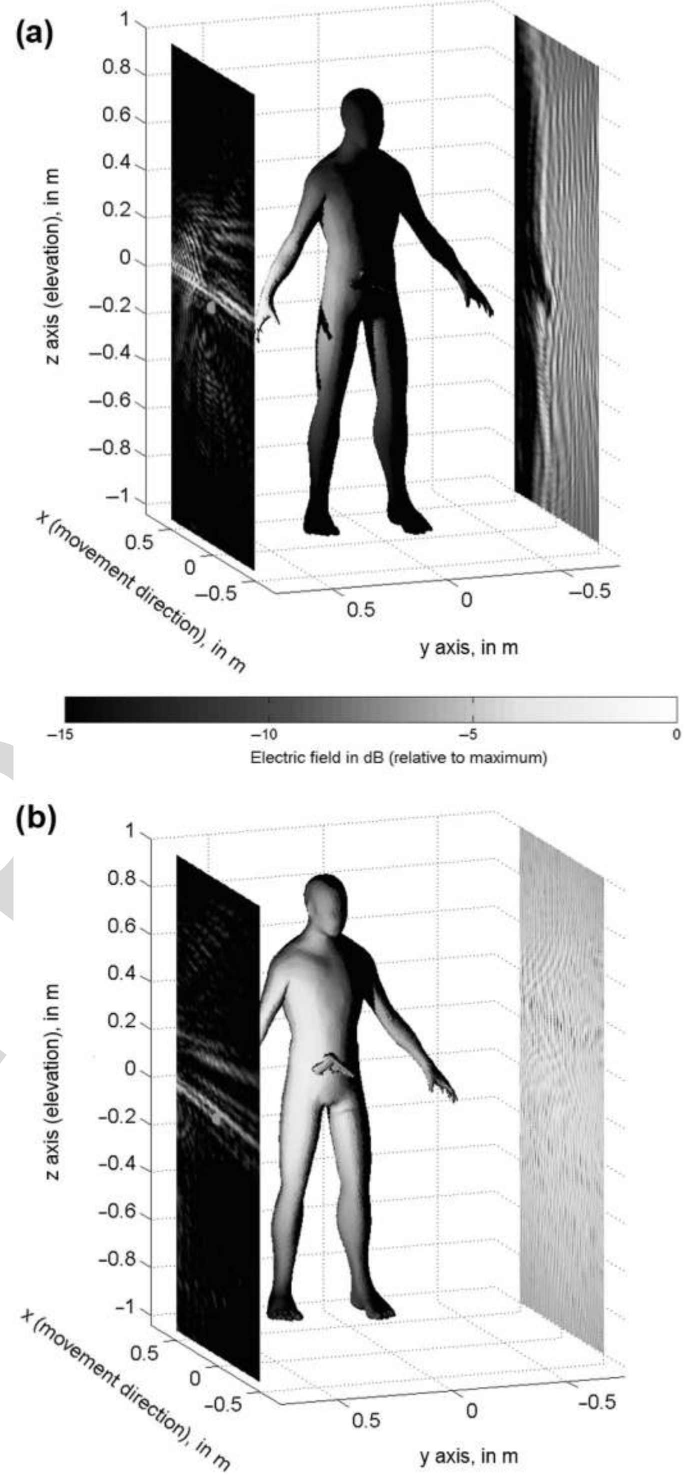

Fig. 13. Examples of human body illumination using one transmitter (highlighted in green) and scattered field on the array panels when the body model is centered in (a) 0.25 m and (b) 0.75 m.

(BW), from 15 to 30 GHz, is chosen, similarly to the UWB imaging system described in [5]. This BW provides and approximate range resolution of 1 cm, although, for near-field radar imaging, besides the frequency and aperture size, the final system lateral and range resolutions are given by (2) and (3) of [20], respectively.

Hallway scanner dimensions have been selected to provide a resolution similar to other mm-wave scanners, as shown in Table I. It must be reminded that the number of receiving elements can be reduced in the hallway system.

Concerning processing time, the fastest operational mm-wave imaging systems listed in Table I are capable to provide detection results in less than 5 s, so the scanning process can take up to 10 s taking into account that the person needs to be placed in a particular position within the scanner. For the presented system, the overall scanning process would be limited by the time the person needs to go through the hallway.

Three arcs of transmitters, centered at x = +1, 0, and −1 m, and each having 20 elements evenly spaced along y- and z-axes, are considered. For the sake of simplicity, only the ones at −1 and 0 m, depicted in Fig. 12, will be considered to obtain the results in this section. Some of the transmitters are placed on top and below the body to ensure the areas with larger curvature (as the top of the chest and shoulders) are reconstructed.

A physical optics (PO) code [21], [22] in combination with a visibility algorithm [23] has been used to predict the parts of the body model in Fig. 12 that are illuminated by every transmitter. Also, PO provides the amount of scattered field collected on the panels. Thus, it is possible to evaluate if a certain layout of transmitters is capable of illuminating the entire person after crossing the hallway and to estimate the field scattered by the illuminated areas on the receiving panels. For these simulations, the human body is assumed to behave as a PEC in the 15–30-GHz frequency band.

As an example, Figs. 13 and 14 show the regions of the human body under test illuminated by two different transmitters, as well as the field received on the lateral panels. Note that, even for a single position of the person in the hallway, different

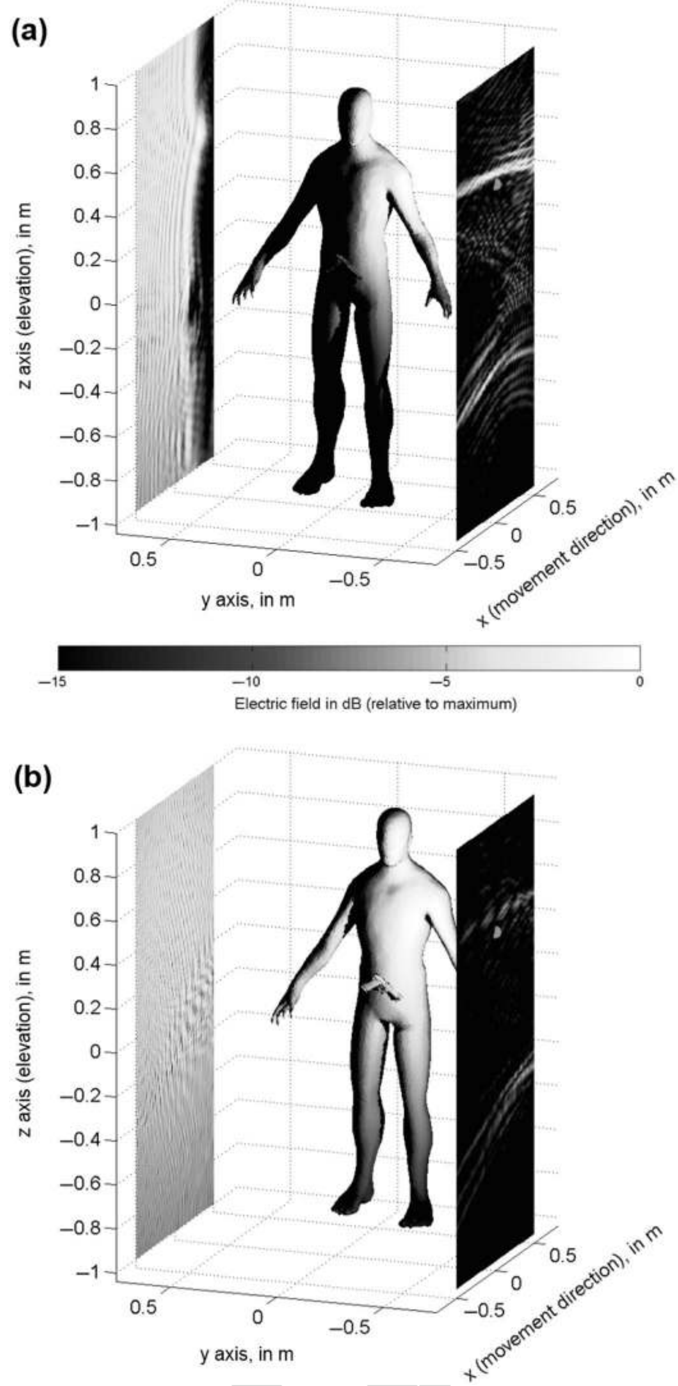

Fig. 14. Examples of human body illumination using one transmitter (highlighted in green) and scattered field on the array panels when the body model is centered in (a) 0.25 m and (b) 0.75 m.

areas of the body are illuminated. This layout increases the amount of information thanks to the spatial diversity of the multistatic illumination.

Regarding the inverse method to create images in this system and due to the large computational cost for the imaging, when the backpropagation is implemented in 3-D, the above-mentioned Fourier-based technique for multistatic imaging [9] has been used. The efficient use of fast Fourier transforms (FFT) provides 3-D whole body imaging in almost real time using conventional hardware.

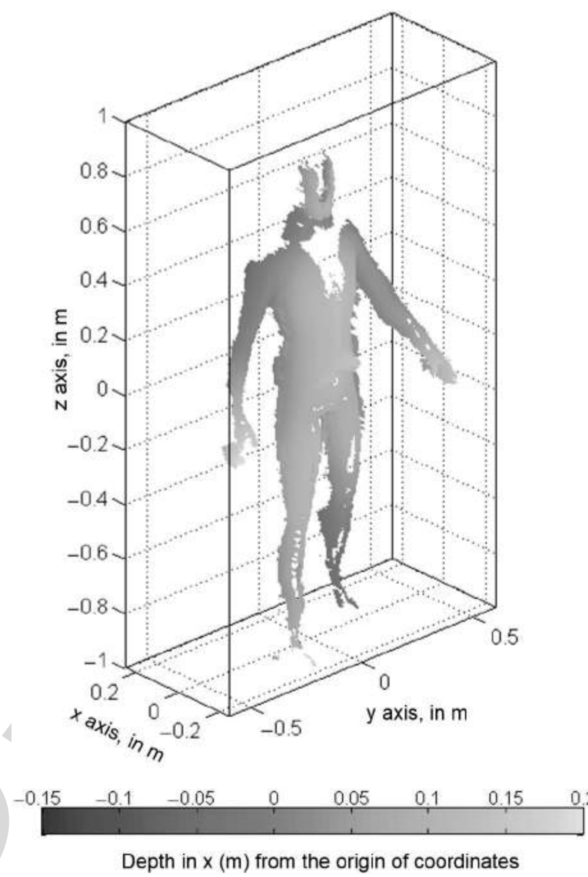

Fig. 15. Person placed at x = 0.25 m. Recovered human body and concealed object geometry from backpropagation imaging.

As an application example to show the performance of the proposed configuration, an OUT consisting on a person carrying a concealed weapon in the belt has been considered. For the sake of simplicity, only two positions are analyzed: person standing at x = 0.25 m and at x = 0.75 m. In this example, the goal is to clearly illustrate the different nature of the multistatic information collected on each position, rather than a rigorous reconstruction of the whole body.

For every position, transmitter, and receiving panel, the amount of data to be processed is: 201×401 spatial samples $\times$ 121 frequency samples ($= 9.75 \times 10^6$ scattered field samples), which also determines the number of imaging points in the case of Fourier-based imaging [9]. A workstation with 32 cores at 2.1 GHz and 128-GB RAM was used for data processing. Overall calculation time for every transmitter was 30 s (1200 s total for the 40 used transmitters). The processing has been done using a sequential Matlab code and has not been optimized for real time imaging yet.

Imaging results are depicted in Figs. 15 and 16, corresponding to the person's placement at x = 0.25 m and x = 0.75 m, respectively. Reflectivity points above -25 dB with respect to the maximum are coded in depth according to x-axis, allowing the recovery of the human body profile and potential concealed weapons. Comparison of Figs. 15 and 16 provides a clear example of the on-the-move imaging concept effectiveness. In the case of Fig. 15 (person placed at x = 0.25 m), the human body sides and some areas of the chest are imaged by the system. In

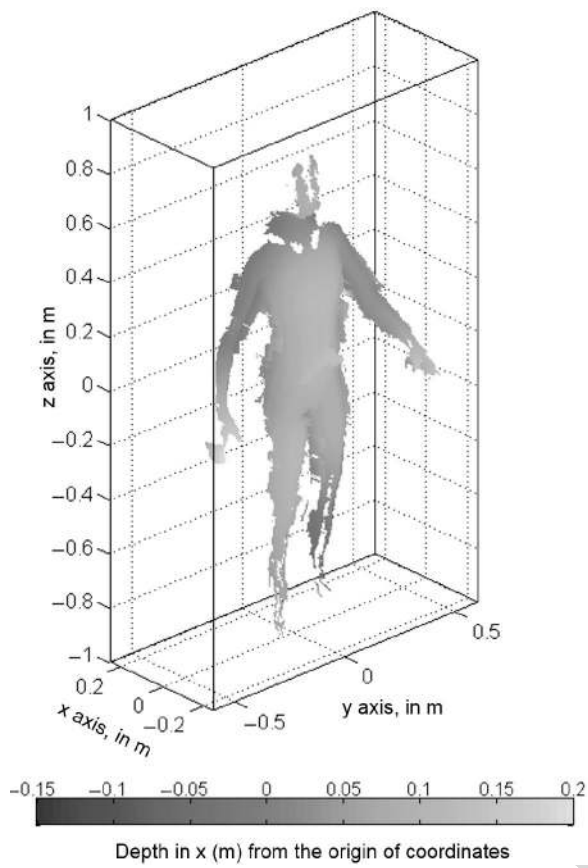

Fig. 16. Person placed at x = 0.75 m. Recovered human body and concealed object geometry from backpropagation imaging.

Fig. 16 (person placed at x = 0.75 m), the top of the chest and the shoulders are recovered.

In the final system, multiple images, as the two presented examples, can be created and analyzed at video rate to detect any possible threats. Algorithms for mesh generation and automatic thread detection, such as the one used in [8], can be applied.

VII. Conclusion

This work presented a novel concept for personnel scanning in airports and other checkpoints. Unlike the current imaging systems, the proposed system allows for continuous movement of the subject while being scanned; this will greatly increase the system throughput when compared with state-of-the-art systems. This improvement is possible thanks to the use of a fully multistatic radar configuration, where some of the transmitters and receivers are separated with a subtended angle relative to the person greater than 90 degrees to capture information from all possible wave incident angles. In this way, the system is able to create a complete contour reconstruction as the person moves inside the system. The use of a small number of transmitters allows for fast image creation as all the transmitters can be sequentially activated in a short amount of time. 2-D and 3-D simulation-based results confirm the good imaging capabilities of the proposed system; 2-D results have also been validated using measurements. Further work will be related with the setup optimization, including the use of sparse arrays and other techniques to reduce the number of receivers, and with experimental validation.

References

[1] IATA. *Checkpoint of the Future. Executive Summary* [Online]. Available: http://www.iata.org/whatwedo/security/Documents/cof-executive-summary.pdf, accessed on Mar. 16, 2015. Q2

[2] S. S. Ahmed, A. Schiessl, F. Gumbmann, M. Tiebout, S. Methfessel, and L. Schmidt, "Advanced microwave imaging," *IEEE Microw. Mag.*, vol. 13, no. 6, pp. 26–43, Sep./Oct. 2012.

[3] S. S. Ahmed, "Personnel screening with advanced multistatic imaging technology," in *Proc. SPIE Defense Secur. Sens.*, 2013, p. 87150B.

[4] D. Sheen, D. McMakin, and T. Hall, "Three-dimensional millimeter-wave imaging for concealed weapon detection," *IEEE Trans. Microw. Theory Techn.*, vol. 49, no. 9, pp. 1581–1592, Sep. 2001.

[5] X. Zhuge and A. Yarovoy, "A sparse aperture MIMO-SAR-based UWB imaging system for concealed weapon detection," *IEEE Trans. Geosci. Remote Sens.*, vol. 49, no. 1, pp. 509–518, Jan. 2011.

[6] D. M. Sheen, D. L. McMakin, and T. E. Hall, "Combined illumination cylindrical millimeter-wave imaging technique for concealed weapon detection," in *Proc. AeroSense*, 2000, pp. 52–60.

[7] Y. Rodríguez-Vaqueiro, Y. Álvarez López, B. Gonzalez-Valdes, J. A. Martinez, F. Las-Heras, and C. M. Rappaport, "On the use of compressed sensing techniques for improving multistatic millimeter-wave portal-based personnel screening," *IEEE Trans. Antennas Propag.*, vol. 62, no. 1, pp. 494–499, Jan. 2014.

[8] B. Gonzalez-Valdes, Y. Alvarez-Lopez, J. A. Martinez-Lorenzo, F. Las Heras Andres, and C. M. Rappaport, "On the use of improved imaging techniques for the development of a multistatic three-dimensional millimeter-wave portal for personnel screening," *Prog. Electromagn. Res.*, vol. 138, pp. 83–98, 2013.

[9] Y. Alvarez *et al.*, "Fourier-based imaging for multistatic radar systems," *IEEE Trans. Microw. Theory Techn.*, vol. 62, no. 8, pp. 1798–1810, Aug. 2014.

[10] G. Yates, A. Horne, A. Blake, and R. Middleton, "Bistatic SAR image formation," *Inst. Elect. Eng. Proc. Radar Sonar Navigat.*, vol. 153, no. 3, pp. 208–213, Jun. 2006.

[11] R. Burkholder, I. Gupta, and J. Johnson, "Comparison of monostatic and bistatic radar images," *IEEE Trans. Antennas Propag. Mag.*, vol. 45, no. 3, pp. 41–50, Jun. 2003.

[12] B. Gonzalez-Valdes, C. Rappaport, and J. A. Lorenzo-Martinez, "On-the-move active millimeter wave interrogation system using a hallway of multiple transmitters and receivers," in *Proc. IEEE Antennas Propag. Soc. Int. Symp. (APSURSI)*, 2014, pp. 1107–1108.

[13] B. Gonzalez-Valdes, C. Rappaport, and J. Martinez-Lorenzo, "On the move millimiter wave interrogation system with a hallway of multiple transmitters and receivers," U.S. Patent 14 562 094, Dec. 5, 2014.

[14] M. Soumekh, "Bistatic synthetic aperture radar inversion with application in dynamic object imaging," *IEEE Trans. Signal Process.*, vol. 39, no. 9, pp. 2044–2055, Sep. 1991.

[15] Y. Alvarez, J. Martinez, F. Las-Heras, and C. Rappaport, "An inverse fast multipole method for imaging applications," *IEEE Antennas Wireless Propag. Lett.*, vol. 10, pp. 1259–1262, Nov. 2011.

[16] D. Andreuccetti, R. Fossi, and C. Petrucci, "An Internet resource for the calculation of the dielectric properties of body tissues in the frequency range 10 Hz–100 GHz," Internet document, 1997 [Online]. Available: http://niremf.ifac.cnr.it/tissprop/, accessed on Sep. 15, 2015, IFAC-CNR, Florence, Italy, 1997, based on data published by C. Gabriel et al. in 1996.

[17] A. W. Morgenthaler and C. M. Rappaport, "Scattering from lossy dielectric objects buried beneath randomly rough ground: Validating the semi-analytic mode matching algorithm with 2-D FDFD," *IEEE Trans. Geosci. Remote Sens.*, vol. 39, no. 11, pp. 2421–2428, Nov. 2001.

[18] C. M. Rappaport, Q. Dong, E. Bishop, A. Morgenthaler, and M. E. Kilmer, "Finite difference frequency domain (FDFD) modeling of two dimensional TE wave propagation," in *Proc. URSI Symp. Conf.*, Pisa, Italy, 2004. Q3

[19] A. Arboleya, Y. Alvarez, and F. Las-Heras, "Millimeter and submillimeter planar measurement setup," in *Proc. IEEE Antennas Propag. Soc. Int. Symp. (APSURSI)*, 2013, pp. 1–2.

[20] S. S. Ahmed, A. Schiessl, and L.-P. Schmidt, "A novel active real-time digital-beamforming imager for personnel screening," in *Proc. 9th Eur. Conf. Synth. Aperture Radar (EUSAR)*, Apr. 2012, pp. 178–181.

[21] J. Meana, J. Martinez-Lorenzo, F. Las-Heras, and C. Rappaport, “Wave scattering by dielectric and lossy materials using the modified equivalent current approximation (MECA),” *IEEE Trans. Antennas Propag.*, vol. 58, no. 11, pp. 3757–3761, Nov. 2010.

[22] L. E. Tirado, J. A. Martinez-Lorenzo, B. Gonzalez-Valdes, C. Rappaport, O. Rubinos-Lopez, and H. Gomez-Sousa, “GPU implementation of the modified equivalent current approximation (MECA) method,” *Appl. Comput. Electromagn. Soc. J.*, no. 9, Sep. 2012. Q4

[23] J. Gutiérrez Meana, F. L. Las Heras Andrés, and J. Á. Martínez Lorenzo, “A comparison among fast visibility algorithms applied to computational electromagnetics,” *Appl. Comput. Electromagn. Soc. J.*, 2009.

Borja Gonzalez-Valdes (M’xx) received the B.S and Ph.D. degrees in electrical engineering from the University of Vigo, Vigo, Spain, in 2006 and 2010, respectively. Q5

From 2006 to 2010, he was with the Antenna and Optical Communications Group, University of Vigo. From 2008 to 2009, he was a Visiting Researcher with the Gordon Center for Subsurface Sensing & Imaging Systems, Northeastern University, Boston, MA, USA. In 2011, he joined the Awareness and Localization of Explosives-Related Threats Center of Excellence, Northeastern University. Since 2015, he has been a Postdoctoral Researcher affiliated with the AtlantTIC Research Center, University of Vigo. His research interests include antenna design, inverse scattering, radar, advanced imaging techniques, and THz technology.

Yuri Álvarez (S’06–M’09–SM’15) was born in Langreo, Spain, in 1983. He received the M.S. and Ph.D. degrees in telecommunication engineering from the University of Oviedo, Gijn, Spain, in 2006 and 2009, respectively.

He was a Visiting Scholar at the Department of Electrical Engineering and Computer Science, Syracuse University, Syracuse, NY, USA, in 2006 and 2008; a Visiting Postdoc at the Gordon Center for Subsurface Sensing and Imaging Systems (CenSSIS)ALERT (Awareness and Localization of Explosive Related Threats) Center of Excellence, Northeastern University, Boston, MA, USA, from 2011 to 2014; and a Visiting Postdoc at ELEDIA Research Center, Trento, Italy, in 2015. He is currently an Assistant Professor with the Signal Theory and Communications, University of Oviedo, Gijn, Spain. His research interests include antenna diagnostics, antenna measurement techniques, RF techniques for indoor location, inverse scattering and imaging techniques, and phaseless methods for antenna diagnostics and imaging.

Dr. Alvarez was the recipient of the 2011 Regional and National Awards to the Best Ph.D. Thesis on Telecommunication Engineering (category: security and defense).

Yolanda Rodriguez-Vaqueiro (S’xx) received the B.S. and M.S. degrees in electrical engineering from the University of Vigo, Vigo, Spain, in 2009, and the Ph.D. degree in electrical engineering from Northeastern University, Boston, MA, USA, in 2015 (after defending her thesis: Compressive Sensing for Electromagnetic Imaging Using a Nesterov-Based Algorithm).

She is a Postdoctoral Researcher affiliated with the AtlantTIC Research Center, University of Vigo. In 2011, she obtained a Research Assistant grant from the ALERT (Awareness and Localization of Explosive Related Threats) Center of Excellence, Northeastern University. She was also granted as a Junior Researcher with the University of Vigo.

Dr. Rodriguez-Vaqueiro was the recipient of the Research-Impact Award by the Department of Electrical and Computer Engineering, Northeastern University (for her work during the Ph.D. studies), the Best Paper Award in the 2012 IEEE Homeland Security Conference, Honorable Mention in the Student Paper Competition in the 2013 IEEE APS/URSI Conference, the Best Paper Award in the 2014 European Conference on Antennas and Propagation, the Burke/Yannas Award to the most original research study in the field of bioengineering in the 2015 American Burn Association (ABA) Meeting, and the Research-Impact Award by the Department of Electrical and Computer Engineering, Northeastern University, in May 2015.

Ana Arboleya-Arboleya received the M.Sc. degree in telecommunication engineering from the University of Oviedo, Oviedo, Spain, in 2009, where she is currently pursuing the Ph.D. degree in telecommunication engineering. Since 2008, she has been a Research Assistant within the Signal Theory and Communications Research Group, TSC-UNIOVI, Department of Electrical Engineering, University of Oviedo. She was a Visiting Scholar in 2014 and 2015 at the Department of Radio Science and Engineering and MilliLab, Aalto University, Espoo, Finland. Her research interests include antenna diagnostics and measurement systems and techniques and high-frequency imaging techniques and applications.

Antonio García-Pino (S’87–M’89–SM’05) was born in Valdemoro, Madrid, Spain, in 1962. He received the M.S. and Ph.D. degrees in telecommunications engineering from the Polytechnic University of Madrid (UPM), Madrid, Spain, in 1985 and 1989, respectively.

From 1985 to 1989, he was a Research Assistant with the Radiation Group, UPM. He joined as an Associate Professor with the Department of Technologies of Communications, University of Vigo, Vigo, Spain, in 1989, becoming Full Professor in 1994. In 1993, he was a Visiting Researcher at the Center for Electromagnetics Research, Northeastem University, Boston, MA, USA. From 2006 to 2010, he was the Vice-Rector of Academic Organization and Faculty, and currently, he is the Director of the International Doctoral School, both at University of Vigo. His research interests include shaped-reflector antennas for communication and radar applications, high-frequency backscattering, computational electromagnetics, and THz technology. In these topics, he has authored more than 100 technical papers in journal and conferences and he has been an advisor of 14 Ph.D. thesis.

Carey M. Rappaport (SM’96–F’06) received the S.B. degree in mathematics, the S.B., S.M., and E.E. degrees in electrical engineering in 1982, and the Ph.D. degree in electrical engineering in 1987 from the Massachusetts Institute of Technology (MIT), Cambridge, MA, USA. Q6

He was a Teaching and Research Assistant with MIT from 1981 until 1987, and during the summers at COMSAT Labs, Clarksburg, MD, USA, and the Aerospace Corp., El Segundo, CA, USA. He joined the faculty at Northeastern University, Boston, MA, USA, in 1987. He has been a Professor of Electrical and Computer Engineering since July 2000. In 2011, he was appointed as a College of Engineering Distinguished Professor. In fall 1995, he was a Visiting Professor of Electrical Engineering at the Electromagnetics Institute, Technical University of Denmark, Lyngby, Denmark, as part of the W. Fulbright International Scholar Program. In the second half of 2005, he was a Visiting Research Scientist at the Commonwealth Scientific Industrial and Research Organisation (CSIRO), Epping, Australia. He has consulted for CACI, Alion Science and Technology, Inc., Geo-Centers, Inc., PPG, Inc., and several municipalities on wave propagation and modeling, and microwave heating and safety. He was the Principal Investigator of an ARO-sponsored Multidisciplinary University Research Initiative on Humanitarian Demining, the Co-Principal Investigator of the NSF-sponsored Engineering Research Center for Subsurface Sensing and Imaging Systems (CenSSIS), and the Co-Principal Investigator and Deputy Director of the DHS-sponsored Awareness and Localization of Explosive Related Threats (ALERT) Center of Excellence. He has authored more than 400 technical journal and conference papers in the areas of microwave antenna design, electromagnetic wave propagation and scattering computation, and bioelectromagnetics, and has received two reflector antenna patents, two biomedical device patents, and four subsurface sensing device patents.

Prof. Rappaport is a member of Sigma Xi and Eta Kappa Nu professional honorary societies. He was the recipient of the IEEE Antenna and Propagation Society’s H. A. Wheeler Award for the Best Applications Paper, as a Student in 1986.

Fernando Las-Heras (M'86–SM'08) received the M.S. and Ph.D. degrees in telecommunication engineering from the Technical University of Madrid (UPM), Madrid, Spain, in 1987 and 1990, respectively.

He was a National Graduate Research Fellow (1988–1990), and he held a position of Associate Professor with the Department of Signal, Systems, and Radiocommunications, UPM (1991–2000). From December 2003, he holds a Full Professor position with the University of Oviedo, Oviedo, Spain, where he was the Vice-Dean for Telecommunication Engineering, Technical School of Engineering, Gijón, Spain (2004–2008). As of 2001, he was the Head of the Research Group Signal Theory and Communications TSC-UNIOVI, Department of Electrical Engineering, University of Oviedo. He was a Visiting Lecturer at the National University of Engineering, Rímac Lima, Peru, in 1996, a Visiting Researcher at Syracuse University, Syracuse, NY, USA, in 2000, and a short-term Visiting Lecturer at ESIGELEC, France, from 2005 to 2011. He held the Telefónica Chair on RF Technologies, ICTs applied to Environment and ICTs and Smartcities with the University of Oviedo (2005–2015). He has authored more than 300 articles published in academic journals and proceedings of international conferences, mainly in the areas of antenna design and the inverse electromagnetic problem with applications in diagnostic, measurement and synthesis of antennas, phaseless techniques, propagation, and microwave to THz imaging and localization, as well as in engineering education.

Dr. Las-Heras was a Member of the Board of Directors of the IEEE Spain Section (2012–2015), and from 2010, he was a Member of the Science, Technology, and Innovation Council of Asturias, Asturias, Spain.

Jose A. Martinez-Lorenzo (M'xx) received the B.S./M.S. degree in 2002 and the Ph.D. degree in 2005 from the University of Vigo, Vigo, Spain, both in electrical engineering.

He joined the faculty at University of Oviedo, Gijon, Spain, in 2004, where he was an Assistant Professor with the Department of Signal Theory and Communications. In 2006, he joined Bernard M. Gordon Center for Subsurface Sensing and Imaging Systems, Northeastern University, Boston, MA, USA. In 2010, he was a Research Assistant Professor with the Department of ECE, Northeastern University. Since August 2013, he has been held a joint appointment with the Departments of MIE and ECE as a Tenure-Track Assistant Professor. He is an Active Member of Awareness and Localization of Explosives-Related Threats (ALERT) a DHS Center of Excellence awarded to Northeastern University. He has authored more than 140 technical journal and conference papers. His research interests include the understanding, modeling, and solving complex engineering problems, with an emphasis on mechanical and electromagnetic sensing and imaging methods for security and biomedical applications (i.e., explosive detection, breast cancer detection).

Prof. Martinez-Lorenzo has received funding from multiple agencies, including: DHS, DARPA, NSF, US Army, and the European Space Agency (ESA). He led the team that won the Best Paper Award in the 2012 IEEE Conference on Technologies for Homeland Security, for the paper on a compressed sensing approach for detection of explosive threats at standoff distances using a passive array of scatterers.

QUERIES

Q1: Please provide captions for Fig. 3 subparts.
Q2: Please provide year of publication for Ref. [1].
Q3: Please provide page range for Refs. [18], [22], and [23].
Q4: Please provide volume number for Ref. [22] and [23].
Q5: Please provide the membership history (year) of the authors Borja Gonzalez-Valdes, Yolanda Rodriguez-Vaqueiro,and Jose A. Martinez-Lorenzo.
Q6: Please provide year of completion for the S.B. degree in Mathematics, S.B., S.M. degrees in electrical engineering of author "Carey M. Rappaport."